Accepted for publication in Polymer Reviews
Published in 2017
DOI: 10.1080/15583724.2017.1309663

Failure assessment, damage development and crack growth in polymer composites via localization of acoustic emission events: A review

G. Romhány[a], T. Czigány[a,b*] and J. Karger-Kocsis[a,b]

[a] Department of Polymer Engineering, Faculty of Mechanical Engineering, Budapest University of Technology and Economics, Muegyetem rkp. 3., H-1111 Budapest, Hungary

[b] MTA-BME Research Group for Composite Science and Technology, Muegyetem rkp. 3, H-1111 Budapest, Hungary

* Corresponding author, email address: czigany@eik.bme.hu (T. Czigány)

ABSTRACT

This review aims at showing how location of the acoustic emission (AE) in loaded polymer composites can be used to get deeper insight in the damage onset and growth, and associated failure events and sequences. Different location methods (experimental and theoretical) are briefly introduced along with the AE characteristics in time-and frequency-domains. Linear (1D), planar (2D) ad spatial (3D) locations of AE are surveyed by selected examples. The cited works demonstrate the versatile use of AE. Apart from damage and failure assessments, AE may be used to reconstruct the crack growth thereby supporting the determination of accurate fracture mechanical parameters. Unlike detection of damage development, the identification of failure mechanisms by considering selected AE signal parameters, including their clustering, is still an open issue. Unraveling the failure mode is, however, a key topic with respect to

structural integrity, residual strength and lifespan expectation of composite parts. Recent major challenge is to establish a reliable, real-time structural health monitoring system making use of located AE events, which are monitored by built-in sensors.

Keywords: acoustic emission (AE), localization, failure, damage, crack growth, fracture mechanics, damage zone, crack reconstruction, signal descriptions

List of symbols and abbreviations:

a_{xi} crack tip position at ith interval

A_0 transversal Lamb-wave

AE acoustic emission

AF aramid fiber

ANN artificial neural network

BF basalt fiber

CA cumulative amplitude

CAI compression after impact

CA_{max} maximum cumulative amplitude

CF carbon fiber

CFRP carbon fiber reinforced plastics

CP cross-ply

CT compact tension

CWT continuous wavelet transform

DCB double cantilever beam

DIC digital image correlation

ENF end-notched flexure

EP epoxy resin

FCP fatigue crack propagation

FEM finite element analysis

FFT fast Fourier transform

GF glass fiber

GFRP glass fiber reinforced plastics

GMT glass mat reinforced thermoplastics

H-N Hsu-Nielson source (pencil lead breaking)

IFSS interfacial shear strength

IT infrared thermography

J-R J-integral resistance

K-R fracture toughness resistance

MMB mixed mode bending

MWCNT multiwall carbon nanotube

NDT non-destructive testing

NF natural fiber

PCL polycaprolactone

PCT parameter correction technique

PE polyethylene

PEEK polyetheretherketone

PEMA polyethylmethacrylate

PET polyethylene terephthalate

PF phenol formaldehyde resin

PP polypropylene

RIM reaction injection molding

RTM resin transfer molding

S_0 longitudinal Lamb-wave

SEN single edge notched

SENT single edge notched tensile

SEM scanning electron microscopy

SGF short glass fiber

SHM structural health monitoring

SSMA single sensor modal analysis

T_g glass transition temperature

TOA time of arrival

TPS thermoplastic starch

TSA thermoelastic stress analysis

UD unidirectional

UP unsaturated polyester resin

US ultrasonic

VARTM vacuum assisted resin transfer molding

WT wavelet transform

ΔCA cumulative amplitude interval

1D linear

2D planar

3D spatial

1. Introduction

The acoustic emission (AE) technique is a passive non-destructive testing (NDT) method for parts undergoing deformation. AE uses suitable sensors to detect transient elastic stress waves generated by rapid release of mechanical (strain) energy from localized sources within the material under stress. The source itself is an “active” (i.e. producing stress waves) flaw (defect) or damage. “Active” means the presence of such flaw, damage which develop, progress at the given loading. This is the major limitation of the AE technique compared to other NDT ones which may also detect “passive” flaws (e.g. ultrasound techniques). Note that AE itself is considered as a “passive" NDT, because it detects defects only while they develop during the test. Among the disadvantages of AE the followings should be mentioned: the applied loading situation is not always reproducible, the energy of the AE events is very small requiring extensive (pre)amplification, and filtering off the background noise is not a simple task.[1] Damage involves various failure events in composites (e.g. matrix cracking, fiber/matrix debonding, fiber pull-out, fiber fracture, ply delamination) along with generation of new cracks and propagation of existing ones. The great advantage of AE is that it can locate the “flaw” over the entire surface of parts and structures without a point-by-point scanning as some other NDTs do.[2,3] Further advantage of the AE technique is that it allows real-time continuous monitoring of the “flaws” also in service of structures. Recall that the part investigated should be under stress. A noticeable benefit of AE is that its detection capability is less dependent on the “flaw” size than in other NDTs, such as ultrasonic (US) inspection. This is due to the fact that the AE signals are released from mechanically activated sources (i.e. being under stress).[4] To make use of the AE phenomenon, the sensors should be able to detect and record minute surface displacements caused when the wave incidents upon the surface of the investigated test coupon or part. A peculiar feature of the AE waves is that they travel in solid plates as Lamb-waves. The waves are bounded by the surface and thus become wave-guided Lamb-waves. They have two propagation modes: in-plane and out-of-plane of the surface. In-plane waves are termed to as extensional, longitudinal, zero-order longitudinal, lowest symmetric or S_0-waves. The out-of-plane wave motion is called transverse, flexural, lowest antisymmetric, zero-order transverse or A_0-waves.[5] Their assessment and differentiation are subject of the modal analysis. The S_0/A_0 ratio depends on the AE source. Source with an out-of-plane motion, such as caused by delamination splitting in advanced composites, produces higher amplitude A_0 than S_0 event.[5,6] An in-plane movement, such as matrix cracking, excites more energies in S_0 than in A_0 mode.

This feature can be exploited to distinguish between the above failure types in advanced composites with suitable ply lay-up, notably in cross-ply arrangement.[5] It is worth of mentioning that usually symmetric Lamb-waves, traveling over long distance, having high velocity and less dispersion, are captured by AE location though this aspect is not explicitly mentioned.

This review is aimed at introducing the recent developments with the application of the AE technique for polymer composites. Emphasis was put on the damage and failure assessments via location of the AE events. This is not only a niche topic in the composite filed but represent the right way to establish real time AE surveillance of the structural integrity ("health") of composite parts and structures during service. Moreover, location of AE seems to be the proper tool to determine the crack onset and growth via which reliable fracture mechanics parameters van be deduced. Note that fracture mechanics parameters are needed for the design of the next generation composite parts. Therefore, the literature was surveyed mostly from 2000 whereby focusing more on showing the possibilities with AE than to deliver an exhaustive review.

2. AE sensors and signal characteristics

The AE sensors should convert the surface displacements, caused by the AE waves, into signals which can be collected and stored. This is commonly solved by piezoelectric transducers converting the surface deformation into voltage signals. On the other hand, works are in progress with fiber optic sensors[7] and other transduction methods[4]. Basic challenge with the AE monitoring is to distinguish between transient (burst-type) and continuous signals. Continuous-type AE is usually disregarded in signal processing. It may originate from friction phenomena within the damage zone of the composites. AE studies always focus on burst-type events because they are linked with the development of "flaws".[7] Characteristics of the transient, burst-type AE signal are introduced along with the related terms in Fig. 1. Note that the signal characteristics (also termed as to descriptors) are time- or frequency-based.[8]

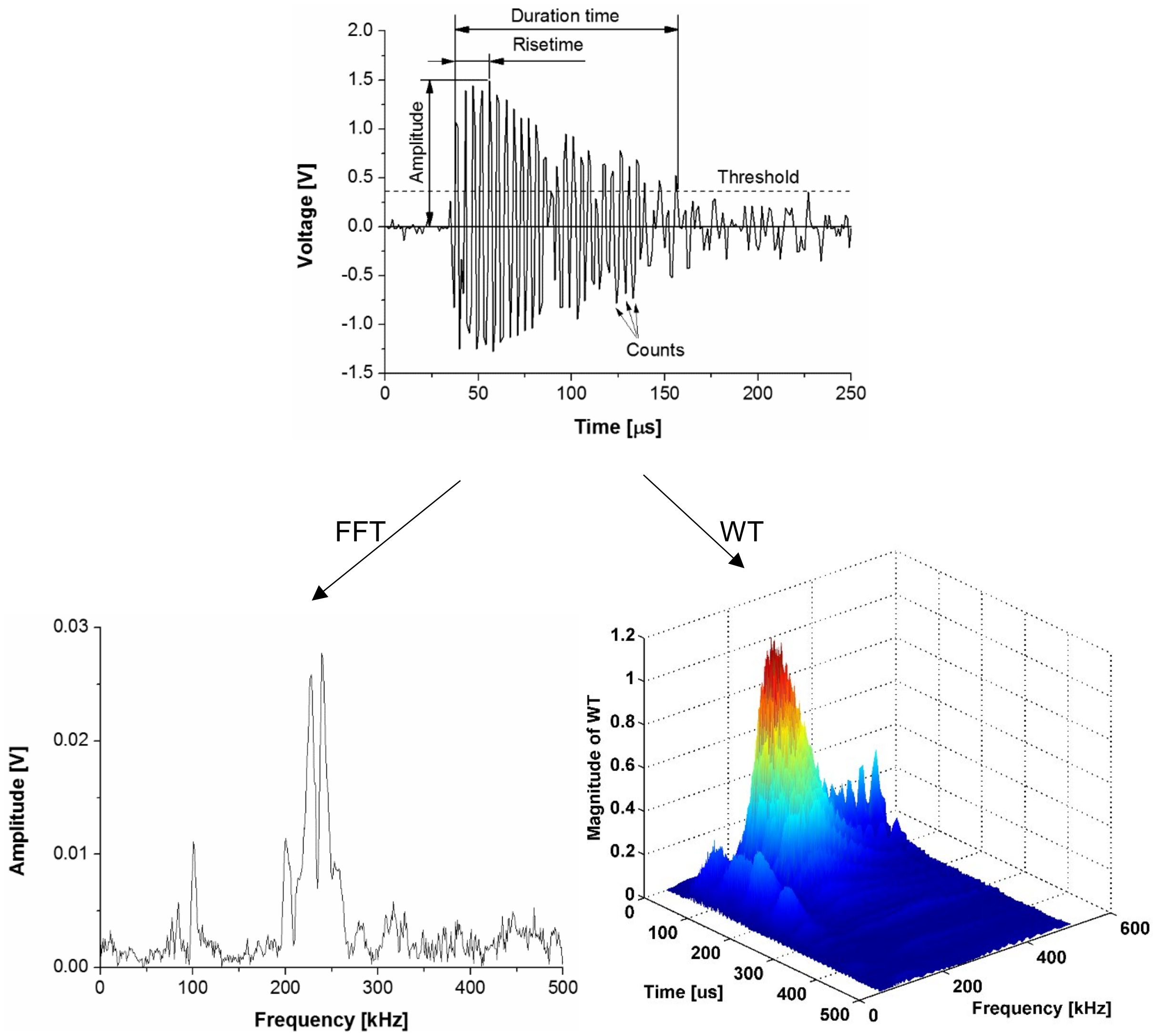

Fig. 1. Characteristics of a recorded burst-type AE event. This figure also shows the frequency- and time-frequency analyses of this burst AE event, captured after surpassing a preset threshold value. Frequency- and time/frequency-analyses were achieved by fast Fourier transform (FFT) and wavelet transformation (WT) techniques, respectively.

Note that continuous signals should be treated always in frequency-domain. The frequency spectrum of the AE event, received by FFT, may be characterized by the dominant frequency range, peak frequency, frequency centroid of gravity, and the like. In the frequency spectrum of the AE event the occurrence time of the corresponding mechanism is unknown. This problem can be resolved by wavelet transformation (WT) that is a time-frequency process method of the AE signals. Similar to FFT also WT may result in further AE signal descriptors. Among the different WTs the Gabor's wavelet proved to be most suited for AE signal processing.[9]

The aforementioned source mechanisms emit AE signals in a wide frequency range, as it will be demonstrated later. Therefore usually broadband, high-sensitivity AE sensors are applied for composite testing. The frequency range is commonly between 100 and 1000 kHz and the sensors have different resonance frequencies. Resonant-type AE sensors are used only when the frequency occurrence of a given failure mechanism is known. The piezoelectric element of the AE sensors is usually a ceramic material. To reduce their size and integrate the sensors better in composite structures works are in progress with polymer sensors. This development is fuelled by the need of resolving the structural health monitoring (SHM) of composites that will be emphasized next.[10] A simple test set-up to detect the AE by one AE sensor is depicted in Fig. 2.

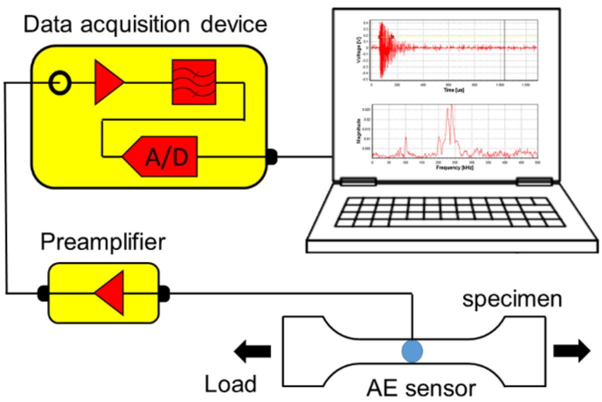

Fig. 2. Simple set-up using a single sensor to detect AE during loading of a test specimen. Notes: the acquisition units contains not only an A/D-converter but also amplifying and filtering options; on the display a burst event along with its FFT spectrum are shown.

The detection and processing of AE events already suggest that some AE characteristics, such as amplitude (cf. Fig. 1) and energy of burst-type events, being affected by filtering, threshold setting and amplification, cannot be compared between different laboratories. This issue is less problematic for frequency-domain characteristics provided that the frequency range and sensitivity of the AE sensors are comparable.

3. Location of AE events and their "processing"

3.1. Source location

To locate the AE source different philosophies exist. The simplest method is based on the first hit (damage onset in the neighborhood) and hit sequence (verification of the source by considering the difference in the arrival times) whereby using a large number of AE sensors. The sensors are positioned in regular arrays. When the first transducer becomes excited then the AE source zone can be located considering the relative position of the other sensors. This may be an acceptable method when the part to be studied is structurally very complex.[11]

The most common approach to locate AE sources is based on the time of arrival (often referred to as time of arrival (TOA)) technique. The AE source is located in the knowledge of the position of the sensors and sound propagation velocity in the given material. This approach assumes that the sound speed is constant in all directions and it is not interrupted between the AE source and each localizing sensor. These prerequisites are, however, not always present in our composite materials. Advanced composites, composed of plies, are strongly anisotropic and thus the AE wave speed becomes also direction-dependent. Wave propagation between the source and sensor may be influenced by holes, thickness changes, and the like (called to "shadowing" effect). As a consequence the location by the TOA algorithm becomes less reliable. Further aspects causing inaccuracy in location are related to the sensing of the TOA (e.g. threshold level, dissimilar frequency characteristics of the sensors).[12]

Nevertheless, TOA location is widely used as referred in the tables 1-3. Using two sensors, located at a given distance apart, determining the time difference in AE signal arrived between sensors 1 and 2 and knowing the AE wave speed, it is possible to define the hyperbola on which the source is located. The exact position of the AE source, however cannot be located. To solve this problem, a third sensor ("triangulation" technique) is added to the array and the source is located by the interception of the hyperbolae between the sensor pairs 1-2, 1-3 and 2-3 – cf. Fig. 3b.[13] Faster location is possible using the interception of circles- cf. Fig. 3c.[14] The above introduced location methods are summarized schematically in Fig. 3.

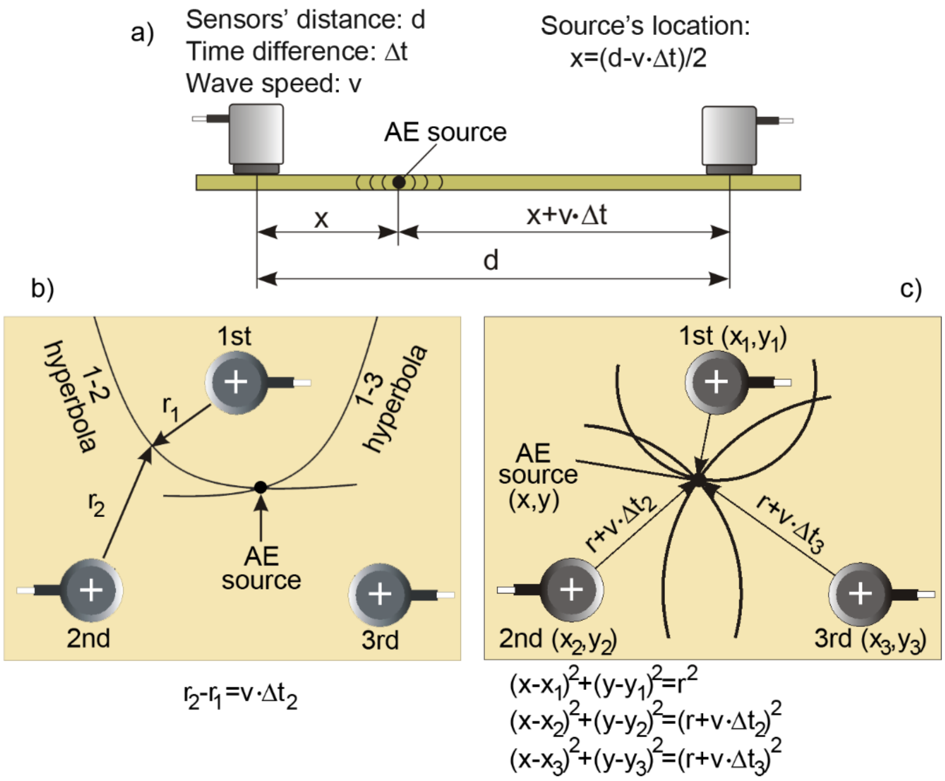

Fig. 3. Linear source location by two (a) and planar source location by three (b and c) sensors. Note: this figure also shows how the source is estimated by the interception of hyperbolae (b) and circles (c), respectively.

Note that due to practical reasons (easier and faster computing) arrays composed of four sensors are preferred. In exceptional cases single sensor modal analysis (SSMA) can also be used for source location. This method exploits the dispersive feature (i.e. frequency dependence) of Lamb-waves. The source is located by measuring the arrival times at given frequencies and determining the speeds of the two dominant wave modes (therefore the attribute “modal”), viz. symmetric and antisymmetric.[13] Recall that both TOA and SSMA are based on the same assumptions, i.e. homogeneous (isotropic) structure, constant wave speed (no direction dependence) and direct wave paths between source and sensors.

A large body of works was devoted to overcome the above limitations. The related developments were fuelled by the necessity to adapt AE location for anisotropic polymer composites. Next we shall report on selected techniques because the comprehensive overview on the various methods (e.g. location refining algorithms[11-13,15-17]) and techniques (e.g. sensors’ arraying) are beyond the scope of this review[4,11,17]. Our intention is namely to show the recent developments in studying the fracture, damage development and crack growth in polymeric systems. It should be born in mind that for the abovelisted tasks the location of the AE is just the tool. Nevertheless, when introducing selected results, achieved by linear (1D), planar (2D) and spatial (3D) locations, respectively, the AE related location technique will be disclosed.

The delta T source location or mapping applies an artificial Hsu-Nielson (H-N) source (pencil break) to acquire TOA data at each sensor pairs within an array. When four sensors are used then six sensor pairs are considered, viz.: 1-2, 1-3, 1-4, 2-3, 2-4 and 3-4. H-N events are generated at different points within the grid covered by the four sensors’ array. Analyzing the difference in arrival time at pairs of sensors allows the construction of a map that displays contour lines of equal arrival time difference for each sensor pairs. By calculating the arrival time difference for each sensor pairs from an actual AE event, a line can be constructed on the former determined time difference map. The AE source is located as a convergence point due to the overlaying results from each of the sensor pairs. Note that this method does not require information on the sensors' positions or the time occurrence of the AE source.[13,16]

Many further location techniques have been recommended. Basics of the inverse filtering or time reversal approach[18,19] is that the input signal can be focused back on the original source if the output received by a transducers' array is time reversed and emitted back toward the excitation site. Work are also in progress to locate the source without knowing the direction dependence of the wave velocity, especially for large structures[20] and make use of signal attenuation characteristics for linear localizations[21].

Nowadays, great efforts are undertaken to detect the onset of a given failure type in real-time. This is the key prerequisite of a trustworthy SHM system for composites. To solve this task, however, not only a reliable location algorithm is needed, but also a proper assignment of AE characteristics to the failure mode of interest.[22]

3.2. Information from located AE

Location of AE is generally aimed at the following aspects: i) assessment of the failure mode and sequence, ii) determination of the damage onset, its extension (zone) and follow its development, and iii) to estimate/reconstruct the crack growth in specimens, parts and structures.

3.2.1. Failure mode and sequence

As shown before in Fig. 1 the burst type AE events have time-and frequency-domain features. In order to assign them to a given failure mode occurred in composites this kind of failure should be exclusively triggered. This is, however, a very big challenge because the various individual failure events are usually superimposed, i.e. they occur simultaneously upon loading. For example in discontinuous fiber reinforced composites fiber/matrix debonding, fiber pull-out and fiber fracture are the individual failure events. Their selective occurrence depends on the fiber layering (with respect to loading), mean fiber length (below or beyond the critical value), fiber/matrix adhesion, loading conditions etc. AE signals from matrix cracking are highly attenuated in polymers having a glass transition temperature (T_g) at room temperature and below, but better recognizable in polymeric composites with matrices of high T_g.

In advanced composites composed of unidirectional (UD) plies of different arrangements the failure scenario is even more complex. Failure events involve transverse (to the load direction) matrix cracking, fiber/matrix debonding, fiber fracture, intra- and interlaminar delaminations (debonding), fiber/roving pull out, different friction phenomena. Their separation is almost impossible, especially in a later stage of damage where continuous AE signal is monitored. Therefore, the failure events and modes should be followed by suitable independent experimental techniques thereby acquiring the AE signals simultaneously.

The other strategy is to use such specimens and mechanical loading modes which cause the solely (or mostly) the targeted failure. For example, AE characteristics can well be traced to fiber fracture when the single fiber fragmentation test (SFFT)[23] is monitored by AE.

Interlaminar fracture test on double cantilever beam (DCB) specimens in advanced composites allows the AE assignment of interlaminar delamination. However, even in these rather simple cases no single AE descriptor can be rendered to the triggered failure because the failure mode is more complex. In case of the single fiber fragmentation test matrix cracking and fiber end debonding, whereas in the crack opening (mode I) DCB test fiber/roving fracture along with matrix cracking may happen at the same time. Nevertheless, researchers tried to assign AE descriptors (selecting either their given ranges or their clusters) to the most probable individual failure events. The basics of the related research strategies were very different. Visual inspection of the failure of short and long glass fiber (GF) reinforced composites and comparison of the registered burst AE events (amplitude, energy) helped to distinguish between debonding, pull out and fiber fracture events.[24] Visual inspection in light and scanning electron microscopy can be considered as a useful tool to assign the captured AE signals to the observed failure modes.[25,26]

Another strategy is to monitor the AE on single and multiply laminates of different lay up (UD alignment in loading and transverse directions, cross-ply (CP)) along with its fiber constituent separately, and deduce the corresponding AE descriptors. These AE parameters are now assigned to the most likely failure mode. In the knowledge of this assignment the AE signals received on a more complex structure, such as filament wound composite pressure vessel, can be distinguished and the probable failure mode estimated.[27]

Suitable model experiments along with finite element analysis (FEM) of the stress state were also useful to discriminate between failure events and their AE characteristics.[28]

From the viewpoint of the AE testing it has to be mentioned that in case of linear location usually two guard sensor are placed outside of the place of interest to filter the background noise. No guard sensors are used when location occurs via an array of three or more sensors.

Assignment of a given failure mode by AE grouping requires an appropriate set of descriptors to be extracted from the AE signals. This method is referred to as pattern recognition that can be made in supervised or unsupervised manner. The former means that the related failure mechanism should be known in advance. This is seldom the case when not "calibrated" using specimens and loading conditions yielding solely the required failure event. Unsupervised pattern recognition implies the whole procedure from descriptors' selection, clustering to cluster validation.[29] For validation purpose *in situ* (e.g. digital image correlation (DIC)) and *post mortem* (e.g. US scanning) techniques may be used, which are sensitive for a given type of failure (delamination in this case[29]).

3.2.2. Damage onset, damage zone and its development

Damage onset and growth are key issues with respect to the expected life span of polymer composite parts. Subcritical damage, by whatever means caused, can often not recognized by bare eyes. On the other hand, this controls the residual load bearing capacity of the composite. For advanced composites, for example, the compression after impact (CAI) test became the standard which is modeling the frequently occurring bird strike in the aircraft industry. CAI tests on composites are increasingly performed with simultaneous AE monitoring in order to get further information the previous indentation damage.[30]

Less demanding composites contain reinforcing mat and fabric reinforcements. Mat-reinforced thermoplastics are usually processed by flow molding. This transfers the originally apparently isotropic structure into anisotropic one. In addition, the stress transfer and thus also the failure mode in glass mat reinforced thermoplastics (GMT) occurs in a quite large area. The representative volume element in fabric reinforced systems also a multitude of the unit cells of the woven fabric. It is obvious that the stress transferring volume in such composites depends on the actual textile architecture (non woven, woven according to different pattern). It turned out that the "equilibrium" damage zone may be several tens of millimeter.[25,31-37]

Accordingly, mechanical tests on specimens with a dimension less than that of the damage zone yield useless data. "Equilibrium" damage zone develops before it starts to propagate. Its size depends also on the loading frequency. The propagation of the damage zone is of great relevance for engineering purpose because in its knowledge the replacement of the failing part can be scheduled.

Determination of the damage zone in fabric-reinforced composites is an excellent tool to check material modifications (e.g. interfacial adhesion) and processing-induced effects. In case of advanced composites efforts are mainly focused on the determination of delamination's onset being the most crucial one with respect to the residual performance of composites.

The damage zone can be estimated by various mathematical weighing function considering the occurrence and characteristic of the AE events monitored during loading of the specimen – cf. Fig. 4a. The located surface was scanned by ellipses (of varied axes and radii)[37,38] or circles[31,32,39], respectively to define that zone which covered an arbitrarily chosen number (usually >75%) of all registered events. Later, this method was refined by considering the surface relating cumulative amplitude[40] and energy[33] thereby still selecting a given percentage of all events to estimate the damage zone – cf. Fig. 4b. The AE results were confirmed by other techniques, such as infrared thermography (IT). Fig. 4b shows that very good agreement was found between the positions of AE- and IT-related damage zones[40] but the extension of the latter was smaller when assessed by IT. This was explained by the difference between the damage and process zone. The damage zone involved fiber/matrix debonding events which were excluded in the IT frames due to their negligible heat rising effect. It is noteworthy that fiber fracture, fiber pull-out and matrix deformation are the major "heat sources" when thermal mapping via IT is selected[41] (Fig. 5).

a)
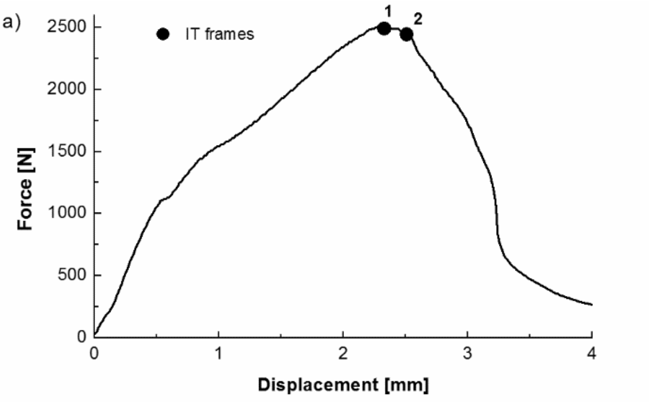

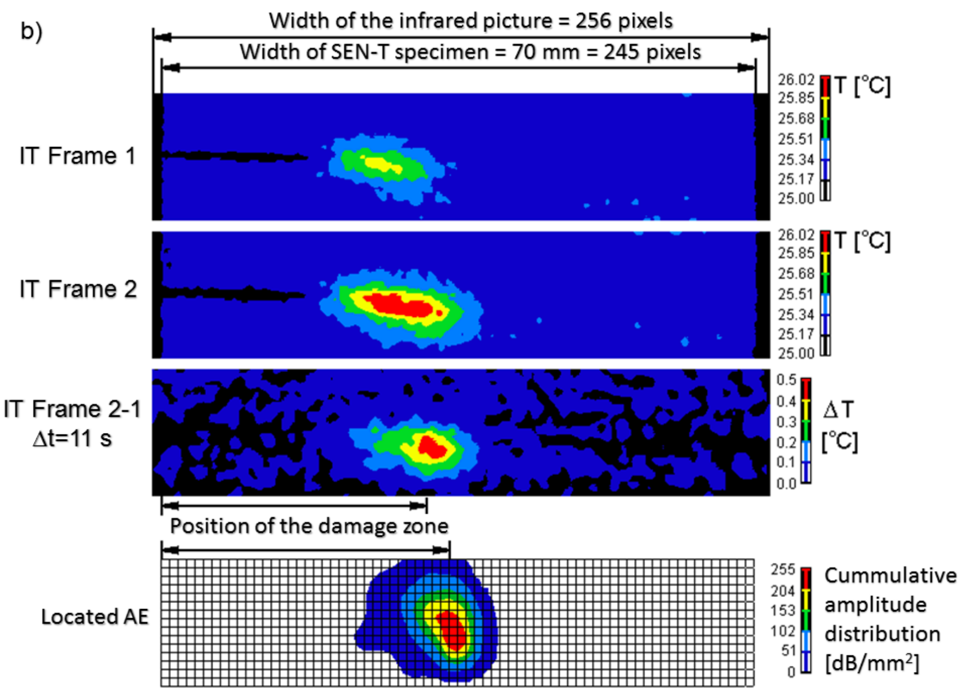

Fig. 4. Load-displacement curve registered on a SEN-T specimen of a thermoplastic starch composite containing 60 wt% flax in CP arrangement (a), and comparison of the damage zones derived from IT and AE measurements (b).[40] Notes: the temperature rise between IT frames 2 and 1 is calculated by considering the corresponding pixels. The AE damage zone covers 90 percentage surface related cumulative AE amplitudes. Reused by permission of Elsevier [40]

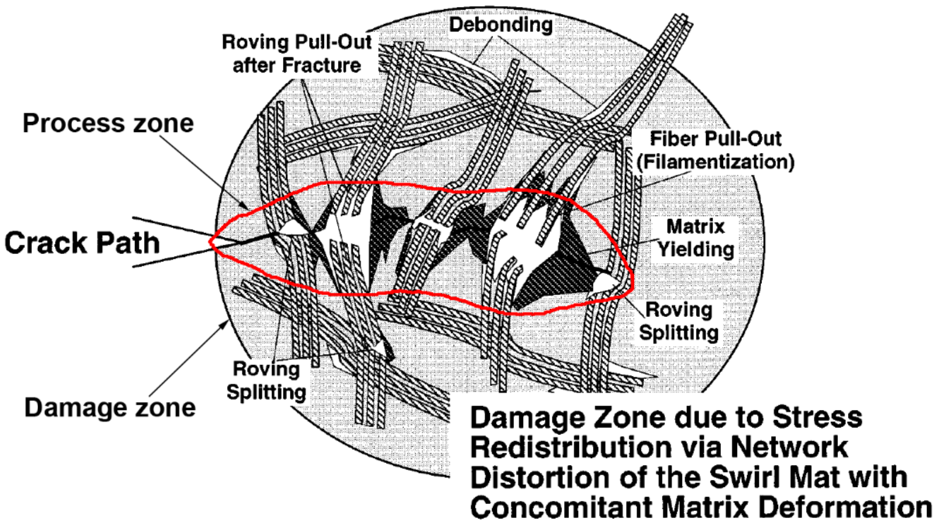

Fig. 5. Damage and process zones in glass mat reinforced thermoplastic composites (GMT) schematically[41]. Note: process zone is marked by red line. Reused by permission of Wiley [41]

3.2.3. Crack growth

In many polymer composites the crack growth can hardly be followed. This may be due to opaque matrix, onset of large damage zone (often characterized by matrix deformation caused stress whitening), complex stress transfer through the reinforcing fabric, cracking in transverse plies "hidden" by longitudinal ones, etc.

Fracture mechanical approaches are gaining acceptance for composites to determine their toughness and resistance to fatigue crack propagation (FCP). Note that all fracture mechanical test use notched specimens. When no sudden fracture occurs the related fracture mechanical concepts consider the energy dissipation during the crack growth.[42] However, to derive fracture mechanical parameters the crack growth should be tracked. Moreover, it would be desirable to follow the crack growth in real-time.

As mentioned before, the mode I delamination behavior is a key issue for advanced polymer composites that is usually measured on DCB specimens. During the test the crack initiation and stable crack propagation values, more exactly the related fracture energy values, should be determined.[43] Visual inspection of the specimens may yield erroneous results due to crack deviation and fiber bridging phenomena. Linear location of the AE with two sensors may contribute to a reliable resolution of both crack initiation and growth.[44,45] This has been demonstrated by Romhány and Szebényi studying the effect of multiwall carbon nanotube (MWCNT) incorporation of EP/CF UD composites.[45] Figure 6a demonstrates that AE events were monitored in the whole linearly localized distance in the loaded DCB specimen. This was attributed to the multiple reflections of the AE signals in the specimen. Accepting that only high amplitude events represent real sources, the located AE events were filtered thereby considering amplitudes only above a given threshold (60 dB) - cf. Fig. 6b.

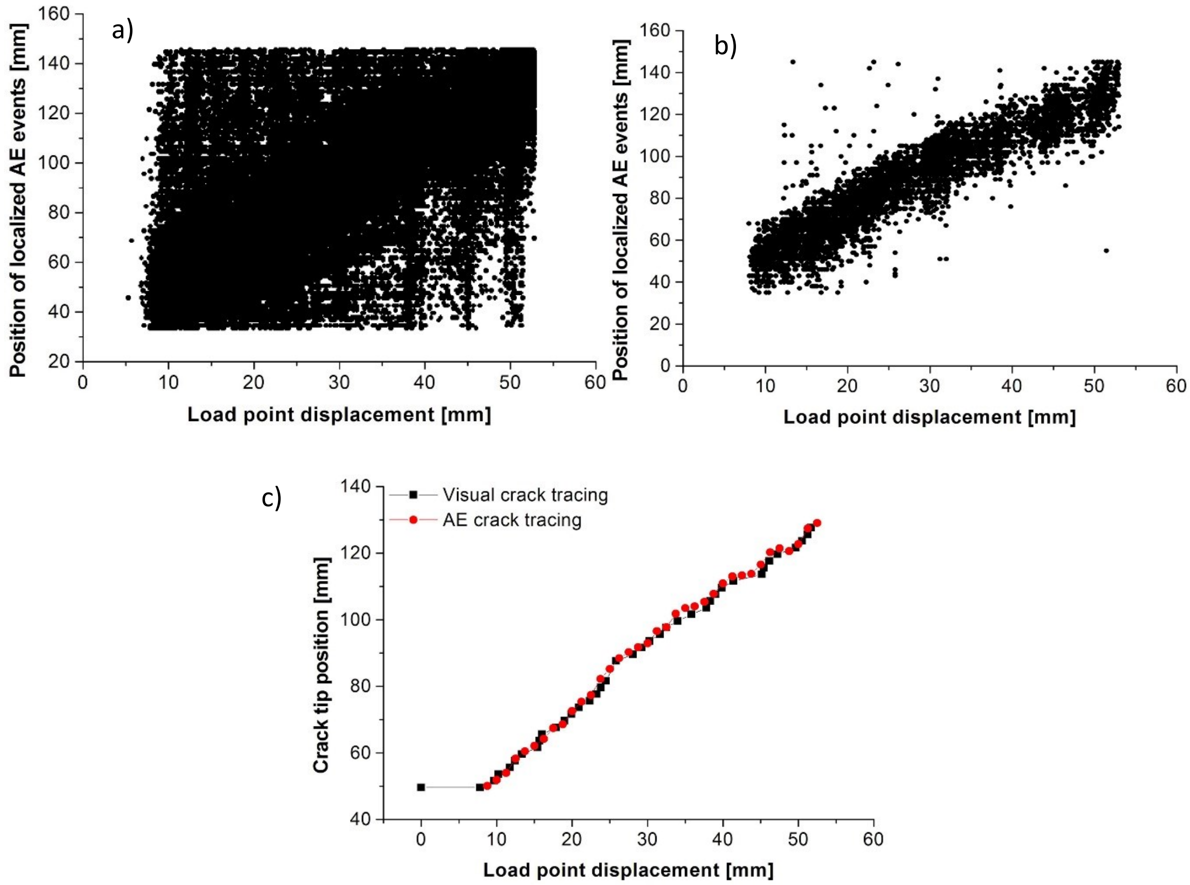

Fig. 6. The localized AE events before (a) and after filtering (b) of a hybrid composite DCB specimen with 0.1 wt% MWCNT. The crack traced by AE and visual inspection is displayed in (c). Reused by permission of BME-PT [45]

The picture in Fig. 6b can be refined further by calculating the average of the crack positions in 15 s long intervals (this corresponds to 1.25 mm of load point displacement). In Fig. 6c the so calculated crack tip positions and the visually recorded positions are compared. The crack tip positions are practically identical, so the AE localization has been verified by the visually observed data.

Moreover, Bohse[44] demonstrated that assuming that delamination involves fiber/matrix debonding and matrix cracking events the mode I fracture energy should correlate with the cumulative energy of the AE events. This prediction has been confirmed.

Reconstruction of the crack growth using located AE events served to determine the J-integral resistance (J-R) curves for various thermoplastic composites containing mat, fabric and UD fibers in CP arrangement. The crack path reconstruction was composed of the following steps. The cumulative amplitude (CA) vs displacement curve was sectioned in equidistance steps (ΔCA), as indicated in Fig. 7. For each section first the smoothed CA distribution has been determined. After that the center of gravity points of the corresponding CA distributions were computed. The center of gravity was assigned to the actual position of the running crack tip. By repeating the above steps the movement of the damage zone, i.e. the crack path, can well be reconstructed. However, caution is requested when selecting the ΔCA sections. If too small ΔCA intervals are chosen, the geometrical places of weight center points do not increase monotonously, hence the crack seems to "heal" in some places. As the crack propagates steadily during loading of the SEN-T specimens the optimum CA has to be chosen iteratively considering that the center of gravity of the damage zone should advance monotonously.

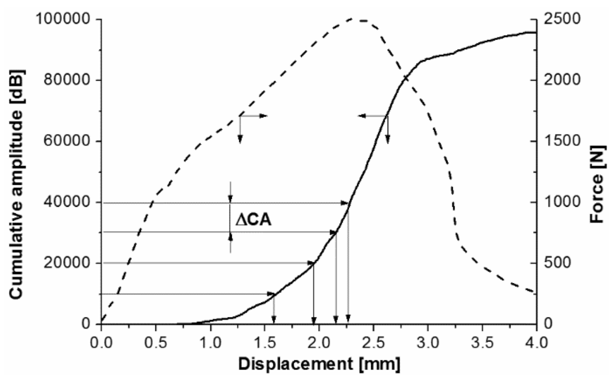

Fig. 7. Sectioning of the cumulative AE amplitude (CA) vs displacement curve of a thermoplastic starch composite containing 60 wt% flax in CP arrangement to get the same ΔCA in each section. Note: this figure also contains the correspondent force-displacement curve. Reused by permission of Elsevier [40]

Note that the crack position before final fracture is never correct. In Fig. 8 the last points marked by A suggest an apparent crack closure. This is due to edge effects. Near to the specimen edge not all events are captured due to the fast fracture. In addition, the center of gravity can never reach the edge of the SEN-T specimen. As a consequence, the points marked by "A" in Fig. 8 should be neglected. For the remaining center of gravity points of the damage zone a Weibull-type function can be fitted as indicated with the continuous line in Fig. 8.

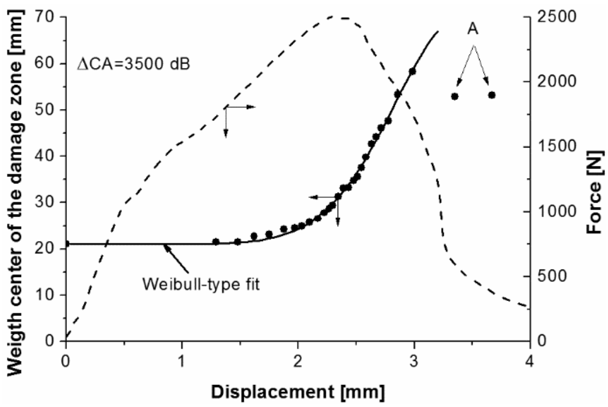

Fig. 8. Calculated crack growth in a SEN-T specimen of thermoplastic starch containing 60 wt% quasi unidirectional flax fiber in CP lay-up. Reused by permission of Elsevier [40]

The steps performed to deduce the crack propagation curve along the ligament are summarized in a flow chart in Fig. 9.

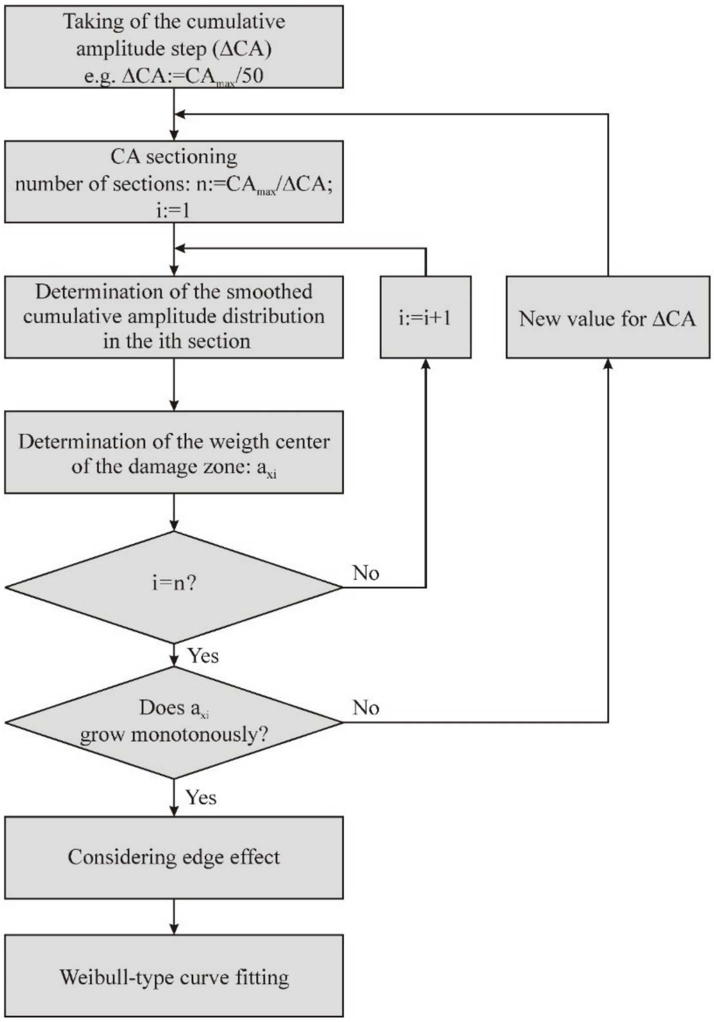

Fig. 9. Determination of the crack path using located AE events. Reused by permission of Elsevier [40]

Examples on the reliability of the crack path tracing using information from located AE events are given in Figures 10 and 11.

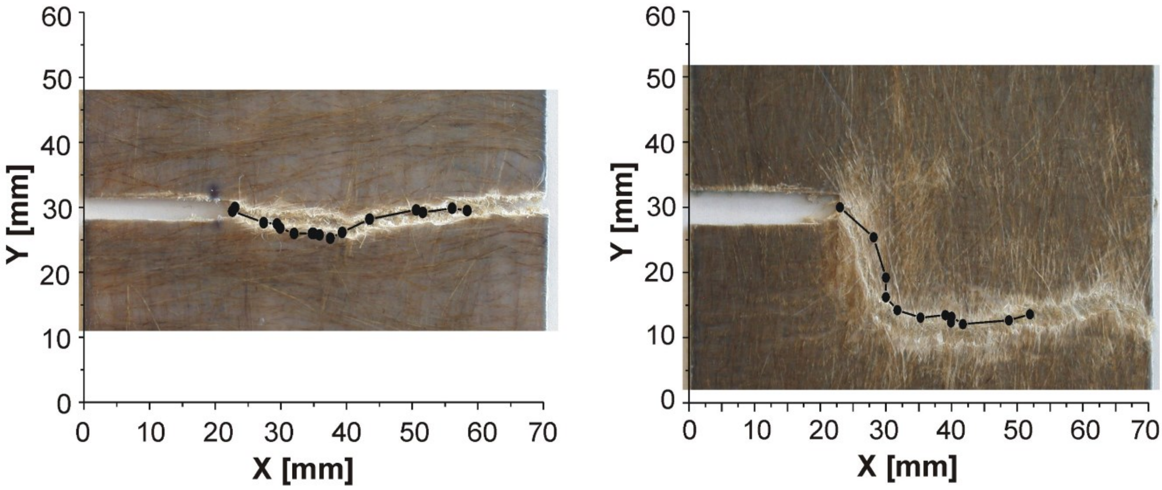

Fig. 10. Comparison of the real fracture path with that of the computed one through location of AE events. Notes: points along the continuous lines represent the movement of the center of gravity of the cumulative amplitudes of AE. Material is a thermoplastic starch with continuous flax fibers in CP lay-up

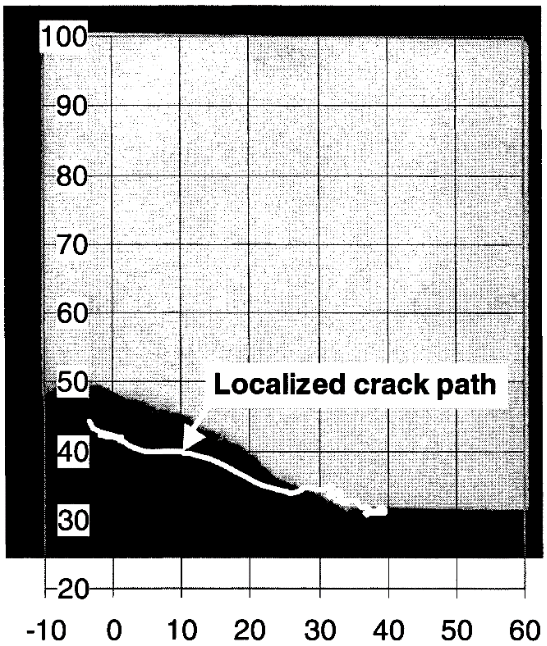

Fig. 11. Comparison of the real fracture path with that of the computed one through location of AE events. Notes: fracture path was computed by considering the advancing the center of gravity of the cumulative energy of AE. Material is a partly consolidated GMT-PP. Deviation between the localized and real fracture planes is due to pull-out events of long discontinuous GF. Scale is in millimeter. Reused by permission of Wiley-VCH [34]

It is noteworthy that great efforts were dedicate to follow the crack growth, similar to the development of the damage zone, by independent techniques, such as IT, DIC, TSA.

Next we shall give a tabulated overview on the use of AE location for failure characterization, damage assessment and crack growth reconstruction in polymer composited. This section will be split for linear (1D), planar (2D) and spatial (3D) locations. The related tables list not only testing-related information but also the major outcome of the cited work. The composites are classified according to their reinforcements as discontinuous, mat, fabrics and UD plies.

It is the right place to mention that an exhaustive review on AE monitoring of the mechanical behavior of natural fiber (NF) composites has been published that covered also result from AE location.[46]

4. Linear (1D) location of AE

1D location of AE has been adapted for different composites. The outcome of selected papers showing the versatile application of AE to get deeper understanding in the failure, damage onset and crack growth are listed in Table 1.

Table 1 Linear (1D) location of AE for composites (note: "-" means "not disclosed")

Composite		Production	Testing	AE set-up, location method	Target of AE use	Results, comments	Ref.
Matrix	Reinforcement						
EP	CF single fiber	embedding	tensile single fiber fragmentation	2 sensors	differentiation in failure events	Distinction between matrix cracking, debonding and CF breakage based on peak frequency (FFT), sequence of these failures concluded from wavelet transformation (WT).	9
EP with different hardeners	CF single fiber with and without electrodeposition	embedding	tensile single fiber fragmentation	2 sensors location by trial and error using pencil lead break	location of fragment	Fragments' length determined by AE and optical microscopy; between them good agreement found. Effects of surface scratches and internal bubbles investigated.	47
PET	SGF	injection molding	tensile loading of single notched specimen	2 sensors (50- 700 kHz), TOA	failure detection during crack growth	Failure events distinguished based on AE amplitudes and frequency analysis utilizing bandpass filters. High amplitude AE corresponded to fiber breakage, whereas low ones to fiber/matrix debonding and matrix fracture. Results supported by polarized optical microscopy and SEM.	48
PP	UD-GF	compression molding	mode I delamination on DCB specimen	2 sensors	failure initiation and sequence	Use of AE location, also for other fracture modes, demonstrated.	44
UP	UD-GF also single fiber composite	hand lay-up	tensile testing in fiber (0°), transverse (90°) and offset (45°) direction	2 sensors (100-1000 kHz), TOA approach	failure identification	Different unsupervised and supervised methods used whereby considering the AE on single fiber microcomposites, as well.	49

Composite		Production	Testing	AE set-up, location method	Target of AE use	Results, comments	Ref.
Matrix	Reinforcement						
EP	UD-GF	hand lay-up	AE energy attenuation at different angles of the GF. No mechanical loading.	1 sensor in three different positions at different times; attenuation approach.	source location	Feasibility of source location making use of Lamb waves' detection shown.	21
EP	CF	almost UD-CF laminate with outer layers transvers to loading	straining along an Euler-Fresnel Spiral jig	2 sensors, TOA	crack onset	1st crack accurately located and confirmed by the penetrant method. Test is useful to determine the critical strain in composite strips.	50
EP with and without MWCNT	UD-CF fabric	hand lamination	mode I delamination on DCB specimen	2 sensors (100-600 kHz), TOA	crack initiation and growth	Crack growth was reconstructed by amplitude filtering of the located events followed by their time averaging within a given time interval – cf. Fig. 6. Good agreement with visual inspection found.	45
toughened EP	UD-CF prepreg	various lay-ups, hand lamination	tensile tests	3 or 4 sensors (2 outers as guard sensors) (50 kHz-2 MHz)	transverse (90°) cracking	Identification of surface and interior transverse cracks using modal analysis. Good correlation between cumulative AE energy and visually observed linear crack density. Peak frequency of FFT alone can hardly be assigned to a specific failure.	51

Composite		Production	Testing	AE set-up, location method	Target of AE use	Results, comments	Ref.
Matrix	Reinforcement						
EP	UD-CF prepreg	UD and CP laminates with different lay-ups	tensile and flexural tests	2 sensors – digital wave (50 kHz-4 MHz), TOA	failure identification and source location	Importance of modal analysis to differentiate between events causing extensional and flexural waves - also with respect to location - emphasized.	52
EP	UD-GF	various lay-ups	tensile tests	6 sensors (2 guard sensors on one surface, 2-2 on both surfaces at mirror positions) (50 kHz-1.5 MHz)	failure types	Different lay-up configurations used to trigger different types of failure and assign them to AE characteristics. Sensor positioning helped to consider flexural waves.	53
EP	UD-CF prepreg	laminates with UD (0°), transverse (90°) and (±45°) lay-ups and sandwich beams	tensile and compression (sandwich) tests	4 sensors (2 outers as guard sensors)	identification of edge delamination	AE results used to refine a laminate theory considering interlaminar shear, tension and compression data. In the companion paper an unsupervised pattern recognition method was developed based on which the onset of delamination could be determined in real time.	22,54
UP	UD-GF; woven GF fabric	hand lay-up	mode I (tensile) on DCB specimens	2 sensors (100-750 kHz)	failure assessment	Unsupervised pattern recognition applied to discriminate between failure events. Selected descriptors were: amplitude, energy, rise time, counts, peak frequency and signal duration. Three signal clusters deduced: matrix cracking, fiber/matrix debonding and fiber failure.	55

Composite		Production	Testing	AE set-up, location method	Target of AE use	Results, comments	Ref.
Matrix	Reinforcement						
EP	CF	different lay-ups	open-hole tensile loaded specimens	2 sensors (50 kHz-2 MHz), TOA	failure assessment	Time-domain parameters (amplitude, energy and cumulative events) considered and failure events discriminated according to amplitude ranges thereby considering the lay-up causing dominant failures.	[56]
EP	UD-GF	CP laminate	tensile fatigue testing along with DIC and IT	2 sensors (200-750 kHz), TOA	failure assessment	Unsupervised pattern recognition used to classify the recorded AE during tensile loading. Descriptors: counts to peak, decay angle, absolute energy and peak frequency. Three stages of fatigue identified and attempt was made to find the related differences in time-and frequency domain AE descriptors. Use of additional NDT techniques (DIC, IT) resulted in deeper understanding of damage development.	[57]
EP	UD-CF fabric	UD and CP laminates by hand lay-up	post-impact flexural tests	2 sensors	failure mode	Peak frequency used to discriminate between matrix cracking, delamination and fiber failure.	[58]
EP	UD-CF	different lay-ups	tensile tests	3 or 4 sensors (2 outers as guard sensors) (50 kHz-2 MHz)	failure mode	AE frequency centroid used to differentiate between transverse matrix crack in the surface and in interior plies. Method recommended for real time damage identification.	[59]
toughened EP	BF+CF woven fabrics	laminates in autoclave	flexural before and after laser shock wave causing delamination	2 sensors (100 kHz-1.5 MHz)	failure mode	Effects of fabric hybridization studied. AE proved to be suitable to detect difference in fiber/matrix adhesion.	[60]

Composite		Production	Testing	AE set-up, location method	Target of AE use	Results, comments	Ref.
Matrix	Reinforcement						
EP	NF (flax, hemp), BF, GF in mats and fabrics	vacuum infusion (vacuum bagging)	post-impact flexure	2 sensors (100 kHz-1.5 MHz)	failure mode	Reinforcement hybridization on the residual properties and related failure studied.	61
toughened EP	CF prepreg	CP laminate, vacuum bag in autoclave	post-impact flexure	2 sensors (100 kHz-1.5 MHz)	failure mode	Frequency analysis was used to differentiate between various failure events.	62
PP	hemp mat+aluminum foil	fiber-metal laminate compression molded	tension and indentation	4 sensors (2 outers as guard sensors)	failure mode	Failure estimated by time domain characteristics (amplitude, counts, duration).	63
EP thermoset PU	UD-GF, UD-CF, noncrimp fabrics	VARTM	tension and tension-fatigue	2 sensors (100 kHz-1 MHz)	failure mode	Pattern recognition technique (k-means algorithm) applied for frequency-related descriptors. Fiber breakage, matrix cracking and interphase failure concluded. Failure always started in the interphase.	64
UP	jute and GF fabrics	RTM, hybrid laminates with different stacking sequence	post-impact flexure + pulse IT	4 resonant sensors (2 outers as guard sensors) (150 kHz)	failure mode	Flexural loading curve sectioned based on the course of cumulative AE events. Time-domain AE parameters (amplitude, duration) used for failure characterization of different hybrid-reinforced composites.	65

Composite		Production	Testing	AE set-up, location method	Target of AE use	Results, comments	Ref.
Matrix	Reinforcement						
EP	short NF and quasi UD NF	hand lamination	tensile and flexure	2 resonant sensors (150 kHz)	failure mode	Loading curves sectioned for four ranges and AE amplitude distributions within determined and traced to individual failure events.	[66]
EP	UD+woven GF skins on PE foam in a sandwich beam	hand lay-up followed by vacuum bagging	mode I delamination	2 sensors (100-750 kHz) Location by pencil lead breakage	correlation between AE events and mode I fracture energy	Acoustic energy-based sentry function used to determine the fracture energy. Good agreement with the traditional data reduction methods.	[67]
UP	hemp fiber mat	hand lamination, compression molding	post-impact flexure	2 resonant sensors (150 kHz)	failure mode	AE amplitude and duration depends on the level of the preceding subcritical impact.	[68]
EP	multiaxial noncrimp GF fabric	hand lamination	tension and flexure	2-3 sensors	failure mode	Knitting pattern of the multiaxial fabric from PET yarn influenced the failure sequence in the composite as observed visually.	[69]
EP	BF+AF fabrics	RTM, hybrid reinforcement with different sequences	post-impact flexure	2 sensors (100 kHz-1.5 MHz)	failure mode and its location	Damage localization after impacts with varying energy. Effect of fabric stacking sequence studied. Difference in failure before and after impact is interpreted by amplitude histograms and amplitude-duration relationship.	[70]
EP	jute+wood felt	hand lay-up, hybridization with various stacking sequence	tensile and flexure	2 sensors (100 kHz-1.5 MHz)	failure mode and its location	Effect of stacking sequence of the hybrid reinforcements studied. Damage localized in flexure. Failure, observed by SEM, traced to AE amplitude and duration ranges.	[71]

Composite		Production	Testing	AE set-up, location method	Target of AE use	Results, comments	Ref.
Matrix	Reinforcement						
EP	BF+GF fabrics	RTM, hybridization with different stacking sequence	post-impact flexure	2 sensors (100 kHz-1.5 MHz)	failure mode and damage location	Effect of stacking sequence on the post impact residual properties studied. Impact caused localized damage. Differences in failure traced to changes in the amplitude histograms. Characteristic failure observed by light microscopy.	72
EP	woven hemp fabric	vacuum infusion	post-impact fatigue (in tension)	2 sensors (100 kHz-1.5 MHz)	failure mode	Wöhler curves determined for impacted and non-impacted specimens. Failure events distinguished based on amplitude ranges. Run of the cumulative AE events as a function of fatigue cycles differed markedly for impacted and non-impacted specimens.	73
EP	BF+CF woven fabrics	RTM, hybridization with different stacking sequence	post-impact flexure	2 sensors (100 kHz-1.5 MHz)	failure mode damage location	Effects of reinforcement hybridization on the residual performance studied. Differences in failure traced to changes in the AE amplitudes and duration times. Failure observed by light microscopy.	74
EP	woven CF prepreg	-	mode I, mode II and mixed mode I+II on DCB, ENF and MMB specimens	2 sensors (100-750 kHz), TOA	crack tip localization	Crack tip position is located by both source location (TOA) and using the cumulative AE energy. Visually observed crack growth and course of the cumulative AE energy had the same trend – between them linear correlation found. Based on this result a single sensor may be enough to locate the crack growth.	75

Composite		Production	Testing	AE set-up, location method	Target of AE use	Results, comments	Ref.
Matrix	Reinforcement						
UP	hemp fiber mat+BF woven fabric	hand lay-up followed by compression molding,hybridization also by stacking sequence	post-impact monotonic and cyclic flexure	2 sensors (100 kHz-1.5 MHz)	failure and damage location	Effects of stacking sequence and subcritical impact energy studied. Impacting narrowed the localized damage zone. Differences in the failure modes were distinguished by AE amplitude and duration time histograms and traced to failure events concluded from fractographic inspection.	[76]
Vinylester	woven GF	VARTM	tensile	2 sensors (25 kHz-1.6 MHz), TOA	damage development followed also optically	AE events characterized by multiparameter descriptors: time domain (amplitude, rise time, peak amplitude) and frequency domain (peak frequency, frequency centroid, weighted frequency) features, and clustered into three groups (transverse cracks, fiber failure and delamination). Failure confirmed by optical inspection and the failure sequence as a function of strain concluded.	[77]
PF	continuous GF with copper strips	compression molding	tensile with DIC	2 sensors, TOA	local damage	Simultaneous measurement of the strain field using DIC and damage location via AE. Maxima in strain field corresponded to increased local AE emission. It was proven that damage development is an inhomogeneous process.	[78]

Considering the information summarized in Table 1, the following conclusion can be drawn:

- 1D location of AE events is an excellent tool to study the failure mode and sequence of single fiber microcomposites. In the single fiber fragmentation test, the fragments can be accurately determined and thus the interfacial shear strength (IFSS) computed.
- To trace the failure mode and sequence, suitable specimens (lay-up, notching) should be selected with simultaneous monitoring the deformation with other non-destructive technique (e.g. DIC, optical microscopy). Nonetheless, it is inevitable to use adequate pattern recognition technique for clustering the suitable AE parameters and trace them to the most likely failure event.[79]
- 1D location is straightforward method to detect the crack initiation and follow the crack growth in fracture mechanical delamination tests (mode I, mode II, mode III and mixed modes). Determination of the initiation delamination using AE features will be pushed forward whereby trying to adapt various clustering for time-scale[80], and novel techniques (e.g. Hilbert transform) for frequency-scale descriptors.[81,82] FEM will be intensively used for validation of the AE results.[83] Efforts will be devoted to estimate the related fracture energy values from AE measurement alone (e.g. sentry functions).[81,84]

5. Planar (2D) location of AE

The introduction of selected papers in Table 2 is following the scheme used in Table 1., viz. advanced composites precede the textile fabric reinforced ones.

Table 2 Selected papers using 2D location of AE for the failure and damage assessment in polymeric composites (note: "-" means "not disclosed")

Composite		Production	Testing	AE set-up, location method	Target of AE use	Results, comments	Ref.
Matrix	Reinforcement						
EP	UD-CF, cross-ply	-	H-N source location TOA of Lamb waves of 300 kHz	2 resonant sensors	source location	Method using the TOA of both S_0 and A_0 Lamb waves developed.	6
PEEK	laminate from UD-CF prepreg	-	high-velocity transverse impact+ shearography and US C-scanning	3 broadband sensors	failure assessment	AE energy, amplitude and count correlated with the impact energy and thus with the damage caused.	85
TPS/PCL blend (MaterBi®)	quasi UD flax, CP laminate	film stacking (compression molding)	tensile test on SEN-T specimen + IT	4 broadband sensors (100-600 kHz), TOA	damage development+ crack growth	Crack growth reconstructed by movement of the center of gravity of the cumulative AE amplitude. Good agreement between the positions of the located AE and IT damage zones. Reconstructed crack growth use to determine the J-R curve. Initiation J-integral of the composite first decreased before passing the matrix value above 40 wt% flax content.	40
EP	CF laminate	-	tensile test, synchronized AE+IT	4 resonant sensors (200 kHz)	failure mode	IT synchronized with AE sensing to measure the depth of discrete failure events (buried thermal source).	86

Composite		Production	Testing	AE set-up, location method	Target of AE use	Results, comments	Ref.
Matrix	Reinforcement						
EP	UD-CF based laminate	autoclave curing	tensile test on center-notched specimen, US C-scanning	4 sensors + 4 additional ones on collocated points on the opposite side; triangulation	location and failure mode	Location according to the best-matched search method using the cumulative number of AE. Matrix cracking and delamination in different directions deduced from angular amplitude patterns. Confirmed that matrix cracks are dominated in S_0-, whereas delaminations in A_0-mode. Model for SHM proposed.	[87]
EP	laminates with different lay-ups from UD-CF; also sandwich	-	impact source location	6 sensors (filtered 200-400 kHz), new TOA method	location	Location based on the differences of stress wave measured by 6 sensors. Continuous wavelet transform (CWT) scalogram used to identify the TOA of flexural A_0 Lamb mode. The new method does not need the *a priori* knowledge of the anisotropy group velocity of AE, the lay-up and thickness of the composite.	[88]
EP	UD-CF laminate	vacuum bagging/autoclave	source location	3 resonant (150 kHz) sensors, TOA	location	Location by virtually trained artificial neural network (ANN) considering the differences in TOAs between the sensors.	[89]
EP	UD-CF in CP lay-up	-	fatigue tensile test on circular center notched specimen+ thermoelastic stress analysis (TSA)	4 broadband sensors (125-750 kHz), delta T mapping	damage location	Damage location (cumulative AE events) after given fatigue cycles using traditional TOA and delta T mapping. Accuracy of delta T mapping is the higher the further is the failure from the central notch – validated by TSA.	[12]

Composite		Production	Testing	AE set-up, location method	Target of AE use	Results, comments	Ref.
Matrix	Reinforcement						
EP	laminate composed of UD-GF in a given stacking	-	direction dependence of AE waves and testing under flexure	9 resonant (150 kHz) sensors for AE wave propagation and 4 for location	AE waves' anisotropy and damage development	Layer stacking on AE velocity and attenuation determined. Damage development followed by location of the AE. The amplitude distribution of the AE served to deduce the failure mode and sequence. Amplitude correction considering attenuation decreased the number of matrix cracking and increased the fiber/matrix debonding and friction events. This was supported by visual inspection.	90
EP	UD-CF laminate	vacuum bagging/autoclave	source location	3 sensors (triangulation), TOA version	source location	Mathematical model to compare and minimize the measured and predicted TOAs. Extensional AE wave speed calculated based on the properties of the UD laminate.	91
EP	UD-CF prepreg in CP arrangement	autoclave	tensile fatigue before and after subcritical transverse impact matrix cracking caused by cutting mid section 0° layers + US C-scanning	5 sensors filtering 95 kHz-1 MHz, delta T mapping	damage location and failure mode	ANN-supported AE events' classification used. Delamination became an active AE source after impact even when it did not grow. Delamination was always associated with matrix cracks. Damage/failure development supported C-scans.	92

Composite		Production	Testing	AE set-up, location method	Target of AE use	Results, comments	Ref.
Matrix	Reinforcement						
EP	UD-CF prepreg, CP arrangement	-	buckling with DIC and US C-scanning	3 (100 kHz-1 MHz)+5 (125 kHz-750 kHz) broadband sensors, delta T mapping	failure mode	AE signals classified by ANN, unsupervised waveform clustering and corrected measured amplitude ratio. All the above methods resulted in 2 classes: matrix cracking and delamination.	5
EP	UD-CF prepreg, CP arrangement	autoclave	repeated subcritical transverse impacts of the plate with center crack	5 broadband sensors (100 kHz-1 MHz), delta T mapping, PCT mapping	failure mode	Parameter correction technique (PCT) proposed that can be considered as an advanced version of delta T mapping.	93
EP	UD-CF prepreg, CP arrangement	-	buckling (uniaxial in-plane compression)+DIC and US C-scanning	3+5 broadband sensors, delta T mapping	failure mode	AE data subjected to unsupervised multivariable clustering (k-means, Fuzzy C-means) to identify damage mechanism. Failure starts with matrix cracking before final damage by delamination.	29
CFRP (not disclosed in detail)		-	tension fatigue on SEN specimen	3 broadband sensors, TOA	damage location and failure	Course of the cumulative AE hits analyzed as a function of cycle time. Change in failure given by the corresponding AE amplitude distributions.	94
GFRP			tension fatigue on notched specimen+ strain gages	4 sensors, TOA	damage location and crack growth	Fatigue crack growth estimated trough the AE energy distribution plots.	95

Composite		Production	Testing	AE set-up, location method	Target of AE use	Results, comments	Ref.
Matrix	Reinforcement						
EP	laminate from UD-CF prepreg with a given stacking	-	impact source location	arrays composed of 7 or 8 sensors, TOA	source location	Nonlinear Kalman-filtering methods used to estimate the source in anisotropic polymer composite.	15
PEMA	weft-knitted CF fabric	hot pressing	tensile test on SEN specimen+IT	4 broadband sensors (20 kHz-1 MHz), TOA	damage development and growth	Damage zone estimated by a weighing procedure. This involved the surface (x,y) scanning of the localized area with 5 mm diameter circles and plotting the relative amount of all located AE events in z-direction. Large damage zone found the extension of which was reduced by increasing knit layers.	31
PET	GF fabrics, swirl mat, weft knit and woven	autoclave; from commingled yarns	tensile test on SEN specimen+IT	4 broadband sensors (20 kHz-1 MHz), TOA	damage development and growth	Direction-dependence of damage development investigated. Damage zone size estimated by a weighing procedure circle scanning of the located surface and plotting the relative proportion of the AE events covered in Z-direction. This resulted in 3D contour plots. IT-based damage zone was smaller than AE-based one. This was explained by assuming that IT is sensitive for the process, whereas AE for the overall damage zone.	32

Composite		Production	Testing	AE set-up, location method	Target of AE use	Results, comments	Ref.
Matrix	Reinforcement						
PP	GF mat (swirl, discontinuous) (GMT-PP)	flow molding	tensile test on SEN specimens	4 broadband sensors (20 kHz-1 MHz), TOA	damage zone, failure mode and crack growth	Damage zone determined by truncation of the surface related cumulative AE energy plots. Crack path estimated by movement of the center of gravity of the AE energy in consecutive time interval. Result used to recalculate the fracture toughness. Failure deduced by sectioning the related load-displacement curves and considering the AE amplitude distribution within.	33
PP	GF mat	papermaking process with partial consolidation	tensile test on SEN specimens +IT	4 broadband sensors, TOA	damage zone, failure mode, crack growth	Damage zone deduced by weigh average (bell-shape function) AE energy mapping. Crack growth traced by the movement of the center of gravity of the AE energy in different time intervals. Results used to determine the fracture toughness resistance (K-R) curves. Released surface heat energy from IT compared with that of the cumulative AE energy. Linear correlation was found between the AE energy release rate and strain energy release rate.	34,96
PP	jute cloth (jute treatment and polymer compatibilizer)	film stacking followed by compression molding	tensile test on SEN specimen	4 broadband sensors, TOA	damage zone, failure mode	Effects of interfacial modifications and jute layers reflected in the surface size of the located AE events and amplitude distributions in different sections of the loading.	97

Composite		Production	Testing	AE set-up, location method	Target of AE use	Results, comments	Ref.
Matrix	Reinforcement						
Nylon RIM	GF swirl mat	reaction injection molding (RIM)	tensile test on CT specimens+optical microscopy	4 broadband sensors (20 kHz-1 MHz), TOA	damage zone, failure mode	Simultaneous monitoring of the failure by AE and light microscopy lead to reliable discrimination between the observed failure and burst AE characteristics (amplitude, energy). Failure events and sequence determined in different sections of the loading (both fracture initiation and growth) of the specimens. Damage development determined by considering that surface which covered more than 95% of the located AE events in the given loading section.	[25,35]
Nylon RIM; PP	GF mat	RIM, film stacking with compression molding	tensile test on CT specimens+optical microscopy	4 broadband sensors (20 kHz-1 MHz), TOA	damage zone, failure mode	Toughness depended on the deformability of the mat in the given matrix. The size of the damage zone may be as large as 30 mm in diameter. This requires to use specimens with adequate dimensions for (fracture) mechanical tests. As criteria to the damage zone the minimum surface of that ellipse considered which contained >=75% of the located AE events. Weighing of the located AE events occurred by circle scanning.	[36]

Composite		Production	Testing	AE setup, location method	Target of AE use	Results, comments	Ref.
Matrix	Reinforcement						
PP	GF mat (swirl)	hot pressing at different conditions	tensile test on CT specimens+IT, optical microscopy	4 broadband sensors (20 kHz- 1 MHz), TOA	damage, failure mode	AE based damage zone (minimum surface of ellipse with a given percentage of located AE events) was much larger than the stress-whitened zones by optical microscopy or IT-related one. Difference is explained by assuming that optical microscopy reflects matrix deformation, in IT measurement fiber pull out and fracture events are also involved whereas in located AE also far range fiber/matrix debonding events are also at work. Changes in the failure mode analyzed by AE amplitude histograms representing different loading sections. This was supported by in situ optical microscopic results.	[37,38]
UP	jute fabric	RTM	post impact flexure+TSA	4 sensors, TOA	damage, failure mode	Damage development studied as a function of subcritical impact energy and level of flexural loading. Burst AE signal parameters (counts, duration, amplitude) considered.	[98,99]

Composite		Production	Testing	AE setup, location method	Target of AE use	Results, comments	Ref.
Matrix	Reinforcement						
PP	GF knit commingled with PP yarn	hot pressing using knitted fabrics produced from commingled yarn	tensile test on SEN specimens	4 broadband sensors (20 kHz- 1 MHz), TOA	damage, failure mode	Effects of reinforcement content and fiber/matrix adhesion (sizing, coupling agent) studied. Damage zone given by the ellipse covering >=80% of the located AE events. 3D contour plots produced by weighing the located events through scanning with circle. Size of the damage zone reduced owing to improved fiber/matrix adhesion.	39
PP	flax carded mat	film stacking, compression molding	tensile test on SEN specimens	4 broadband sensors (100-600 kHz)	damage, failure mode	3D contour plots constructed by weighing the located AE events through scanning with a circle of 5 mm radius. Fiber content affected the damage zone less than moisture. Fracture toughness correlated with cumulative AE events.	100
EP	CF woven fabric	film stacking, compression molding	source location	3 broadband sensors (100 kHz- 1.2 MHz), TOA with wave mode analysis and wavelet transform	source location	Closely arranged triangular array used with a new location algorithm to locate the source.	17

Composite		Production	Testing	AE setup, location method	Target of AE use	Results, comments	Ref.
Matrix	Reinforcement						
Matrix	Reinforcement	film stacking, compression molding	tensile test on SEN specimens	4 broadband sensors (100-600 kHz), TOA	damage development, failure mode	Damage development was followed by located AE, IT and visual inspection simultaneously. The crack growth was reconstructed based on AE and IT results and compared with the visually tracked one. The fracture behavior was characterized by the J-R concept. The size of the damage zone according to the cumulative amplitude distribution of located AE (cf. Fig. 4) was at about 20 mm. Effect of flame retardant also investigated.	101

The results in Table 2 can be summarized as follow:

- Reliable, accurate source location is still a key research topic. The major target is, however, not only to locate the failure onset but to trace it to that failure mode which influences the residual performance. Goal of the related efforts is to establish a real-time (i.e. *in situ*) SHM system.
- Location of AE proved to be a useful tool to estimate the size of the damage zone and its development during mechanical loading. The related AE measurement is nowadays combined with other NDT methods at the same time in order to get deeper insight in the occurring fracture/failure.
- Reconstruction of crack growth in composites using different approaches for the located AE events is feasible. This is most helpful to calculate fracture mechanical parameters, especially to create the resistance curves for textile fabric reinforced composites. Recall that in the large damage zone of textile reinforced composites the progress of the crack tip can hardly be followed visually.
- Tracing located AE characteristics to individual failure events, types is pushed forward by various pattern recognition techniques. To support the related clustering, AE testing is now performed on specially designed composites the structure of which triggers a given failure mode. This helps us to assign AE parameters to the expected and observed failure properly.

6. Spatial (3D) location of AE

In this section the results of such papers will be introduced whose authors studied the damage/failure in non-flat specimens, parts and constructions. They are listed upon the research objects from less to more advanced, complex composite systems in Table 3. It is the right place to mention that location of AE 3D volume structures requires suitable mathematical algorithms.[102,103]

Table 3 Selected papers using 3D location of AE for the failure and damage development in polymer composite parts and structures (note: "-" means "not disclosed")

Composite part, structure, constituent	Production	Testing part, condition	AE set-up, location method	Target of AE use	Results, comments	Ref.
curved anisotropic composite plate	-	source location	6 sensors in 2 arrays, within the array 3 sensors closely located	source location	New algorithm proposed. The formulation does not require the knowledge of the wave speed in the plate-like structure.	20
pultruded fiber reinforced polymer (not further specified)	pultrusion	rectangular specimens under compression	4 resonant sensors (50 kHz)	failure mode	Effect of thermal conditioning studied and dominant failure modes concluded. Parallel runs between the accumulated AE and mechanical energies found. FEM used for the validation of collapse.	104
all-composite cylinder, plastic liner with filament wound CF/EP shell	CF filament winding	cylinders with and without impact damage, in pressure cycles	5 sensors location by distance-amplitude correction	damage and failure	AE clearly revealed whether or not the cylinder was previously damaged. For periodic inspection of the pressurized cylinders AE detection in one pressure ramp suggested. From loading/unloading tests the failure mode could not be deduced.	44

Composite part, structure, constituent	Production	Testing part, condition	AE set-up, location method	Target of AE use	Results, comments	Ref.
composite cylinder (pressure vessel) composed of aluminum liner overwrapped by CF/EP shell	CF filament winding	cylinders with different damages produced by different curing methods and tested at different temperatures (cryogenic, ambient) in various pressurization schemes	7 resonant sensors (150 kHz)	burst pressure prediction using mathematically modelled AE data	Self-organizing map was used to filtered AE data, traced to four distinct mechanisms whereby considering AE amplitude, duration and energy. Backpropagation neural network and multiple linear regression analyses used to predict burst pressures.	105
pressure vessel: polymer liner overwrapped by CF/EP and GF/EP (outer layer)	filament winding	cut section of cylinders without liner and coupons, tension tests	4 sensors; 2 guard sensors and 2 wide band (100-900 kHz) face-to-face arranged	modal analysis of AE	S_0 and A_0 wave modal contents determined. CWT applied for signal processing prior to clustering to trace the failure mode and sequence	106
aircraft component	-	source location	4 resonant sensors, delta T mapping	source location	Accuracy of delta T mapping compared with that of traditional TOA.	13
CF composite plate with vertical stiffeners and with connecting rivets	-	source location	1 sensor narrow bandwidth	source location	Time reversal approach based on 1-channel AE detection developed. Approach does not require the knowledge of the mechanical properties of the structure and the anisotropic group speed.	18

Composite part, structure, constituent	Production	Testing part, condition	AE set-up, location method	Target of AE use	Results, comments	Ref.
wind turbine blade composed of GFRP shell, shear web and PVC foam core	-	flexure (full-scale) with strain gages	up to 6 resonant sensors (30 and 60 kHz)	damage location	AE source location by energy contour mapping algorithm. AE located damage agreed well with results of strain gage measurement, also confirmed by visual inspection.	107
wind turbine blade composed of CFRP (EP), GFRP (EP) and balsa wood	hand lay-up	static flexure with loading/deloading at different stress levels, additional (+) strain gages	12 sensors arranged in 4 arrays	damage development	Multiple damage areas identified by structural neural system. This method locates the damage on the first hit (wave arrival) – no need of the knowledge of wave speed in the structure.	108
composite tail rotor blade of a helicopter (GFRP, CFRP, foam)	-	impact source location	4 broadband sensors	source location	Imaging technique proposed based on reciprocal time reversal approach. Imaging occurred by virtual focusing procedure without using iterative algorithms or knowing the direction dependent mechanical properties of the structure.	19
helicopter hexbeam (GFRP+aluminum)	-	vibration caused by actuator in the hexbeam with delamination	4 sensors (2-2 positioned on the top and bottom)	damage detection	Different damage detection methods (resonant comparison AE wave propagation) used for testing and the results compared.	109

Composite part, structure, constituent	Production	Testing part, condition	AE set-up, location method	Target of AE use	Results, comments	Ref.
sandwich composite fuselage panels and structures of airplane (CF-EP laminate, honeycomb core)	-	combined loading (internal pressure; hoop, longitudinal and shear loads) of panels and full-scale structures with and without artificial notches+strain gages+DIC+ computer-aided tap test	8 (+3 or 8) sensors broadband and resonant (150 kHz), TOA	damage development and failure	AE signals, which hit at least 3 sensors defined as three-hit events, were considered. AE signal descriptors were separated into subset of events - monitored at given position, loading and time - to trace them to most likely failure modes. It was concluded that AE is a suitable tool to detect and locate the damage onset and growth. However, the traditional AE signal characteristics (burst-type: amplitude, duration, counts, energy; frequency-based: waveform, peak frequency, frequency centroid…) failed to identify and discern various failure types.	[110,111]

Learning from the works introduced in Table 3 can be summed up as follows:

- The complex structure (lay-ups, built in metallic and foam parts, multiple sandwich…) of parts and structures requires the use reliable source location methods. This problem may be solved experimentally (e.g. many sensors in different arrays thereby considering the first hit at one of the sensors) and theoretically (defining algorithms) which do not need a priori information on the anisotropic characteristics (mechanical, acoustical) of the related parts.
- The damage development, and especially its growth, can well be detected and followed by located AE. This has been proven using other techniques such as digital image correlation (DIC), strain gaging, thermography, ultrasonic testing and computed tomography (e.g.[111]).
- Failure mode detection for SHM, especially in real-time, is the most challenging task nowadays. This involves not only the proper failure assignment to adequate AE characteristics but also the incorporation of suitable AE sensors in the structure. Their role is to "supervise" the structural integrity of the structure without sacrificing its mechanical performance.

7. Conclusions

Polymer composites fail by many different failure events. Their occurrence and sequence depend on several factors, such as type/amount of reinforcement, type of the matrix, laminate lay-up, presence of processing-induced "faults", thickness changes, multimaterial structure, previously introduced damage etc. Unlike localized failure detection methods (optical fibers, strain gages) AE is able to detect the onset of failure in far range.

The basic presumption of AE that each failure event generates a stress wave with given signal characteristics and thus the failure can be unequivocally assigned to these characteristics, descriptors. This is, however, not the case by far. AE signals with similar characteristics may originate from different failure sources. AE signals may be superimposed, especially in the final stage of the loading, thereby distorting their characteristics. Nevertheless, simple burst-type AE parameters may be well used for discontinuous fiber[24,112] and mat-reinforced composites[33,34,96] for failure assignments.

However, sophisticated clustering of AE signal characteristics should be used to identify individual damage features[113], and especially for tracking that failure mode which is associated with a detrimental worsening of the performance. Location of the AE activity is of great relevance even when the failure sequence is the object of study because the background noise should be filtered off. For this purpose usually guard sensors are used.

Location of AE is straightforward when the composite has existing damage (manufacturing problem, foreign impact, damage prior service load). Recall that the post-impact tensile or compression performances are considered as key parameters in aerospace composites. The extent of formerly caused damage can be well estimated by locating the AE with 3 or more sensors upon loading. However, the density, relative occurrence of different failure events within the damage zone can hardly be estimated. In this respect FEM may deliver further insight.[114] Though the location itself is a problematic issue (e.g. material anisotropy, signal attenuation, threshold selection, sensor parameters), its solution seems to be an easier task than the failure identification itself. For location of “new” damage different experimental and theoretical approaches are recommended. They differ from one another mostly whether or not the knowledge of the direction dependence of the AE wave is a prerequisite. Those methods which do not require wave propagation data are strongly favored for the structural health monitoring (SHM) of polymer composites with complex structures.

Beneficial results achieved on coupon specimens, planar panels are still to be confirmed in full-scale structures. The present challenge is to incorporate suitable AE sensors in composite parts which do not sacrifice the mechanical performance and are capable to detect damage along with identification of the actual failure in real-time. This would meet all the requirements of a reliable, robust SHM system.

Acknowledgements

This work was supported by the Hungarian National Research, Development and Innovation Office – NKFIH (grant number OTKA K 116070). This work is connected to the scientific program of the "Development of quality-oriented and harmonized R+D+I strategy and functional model at BME" project. This project is supported by the New Széchenyi Plan (Project ID: TÁMOP-4.2.1/B-09/1/KMR-2010-0002).

References

1. Grosse, C.U.; Ohtsu, M., eds., *Acoustic Emission Testing*, Springer-Verlag Berlin Heidelberg, 2008.
2. Kotsikos, G.; Evans, J.T.; Gibson, A.G.; Hale, J. "Use of acoustic emission to characterize corrosion fatigue damage accumulation in glass fiber reinforced polyester laminates*", Polym. Composite* **1999,** *20*, 689-696.
3. Halasz, I.Z.; Romhany, G.; Kmetty, A.; Barany, T.; Czigany, T. "Failure of compression molded all-polyolefin composites studied by acoustic emission*", Express Polym. Lett.* **2015,** *9*, 321-328.

4. Eaton, M.J.; Pullin, R.; Holford, K.M. "Towards improved damage location using acoustic emission", *P. I. Mech. Eng. C-J. Mec.* **2012,** *226*, 2141-2153.

5. McCrory, J.P.; Al-Jumaili, S.K.; Crivelli, D.; Pearson, M.R.; Eaton, M.J.; Featherston, C.A.; Guagliano, M.; Holford, K.M.; Pullin, R. "Damage classification in carbon fibre composites using acoustic emission: A comparison of three techniques", *Compos. Part B-Eng.* **2015,** *68*, 424-430.

6. Toyama, N.; Koo, J.H.; Oishi, R.; Enoki, M.; Kishi, T. "Two-dimensional AE source location with two sensors in thin CFRP plates", *J. Mater. Sci. Lett.* **2001,** *20*, 1823-1825.

7. Mancini, S.; Tumino, G.; Gaudenzi, P. "Structural health monitoring for future space vehicles", *J. Intel. Mat. Syst. Str.* **2006,** *17*, 577-585.

8. Yoon, S.J.; Chen, D.D.; Han, S.W.; Choi, N.S.; Arakawa, K. "AE analysis of delamination crack propagation in carbon fiber-reinforced polymer materials", *J. Mech. Sci. Technol.* **2015,** *29*, 17-21.

9. Ni, Q.Q.; Iwamoto, M. "Wavelet transform of acoustic emission signals in failure of model composites", *Eng. Fract. Mech.* **2002,** *69*, 717-728.

10. Singh, A.K.; Yang, H.; Shen, R.; Justin, G.; Zimmerman, A.T. Polymeric sensors for health monitoring of composite structures, Report AFRL-RX-WP-TP-2012-0396, Air Force Research Laboratory, 2012.

11. Summerscales, J. Acoustic emission source location in fibre-reinforced composite materials, Report ISBN-13 978-1-870918-04-6, Advanced Composites Manufacturing Centre at Plymouth University, 2013.

12. Eaton, M.J.; Pullin, R.; Holford, K.M. "Acoustic emission source location in composite materials using Delta T Mapping", *Compos. Part A-Appl. S.* **2012,** *43*, 856-863.

13. Baxter, M.G.; Pullin, R.; Holford, K.M.; Evans, S.L. "Delta T source location for acoustic emission", *Mech. Syst. Signal Pr.* **2007,** *21*, 1512-1520.

14. Pellionisz, P. Materials and structures examination by acoustic emission (in Hungarian), GTE, Budapest, Hungary, 1992.

15. Niri, E.D.; Farhidzadeh, A.; Salamone, S. "Nonlinear Kalman Filtering for acoustic emission source localization in anisotropic panels", *Ultrasonics* **2014,** *54*, 486-501.

16. Pullin, R.; Baxter, M.; Eaton, M.; Holford, K.; Evans, S. "Novel acoustic emission source location", *J. Acoustic Emission* **2007,** *25*, 215-223.

17. Aljets, D.; Chong, A.; Wilcox, S.; Holford, K. "Acoustic emission source location in plate-like structures using a closely arranged triangular sensor array", *J. Acoustic Emission* **2010,** *28*, 85-98.

18. Ciampa, F.; Meo, M. "Impact detection in anisotropic materials using a time reversal approach", *Struct. Health Monit.* **2012,** *11*, 43-49.

19. Ciampa, F.; Meo, M. "Impact localization on a composite tail rotor blade using an inverse filtering approach", *J. Intel. Mat. Syst. Str.* **2014,** *25*, 1950-1958.

20. Kundu, T.; Nakatani, H.; Takeda, N. "Acoustic source localization in anisotropic plates", *Ultrasonics* **2012,** *52*, 740-746.

21. Hafizi, Z.M.; Epaarachchi, J.; Nizwan, C.K.E.; Lau, K.T.; Iop, in *1st International Conference on Mechanical Engineering Research 2011*, Iop Publishing Ltd, Bristol, 2012, vol. 36, pp. 1-8.

22. Lorriot, T.; Wargnier, H.; Wahl, J.C.; Proust, A.; Lagunegrand, L. "An experimental criterion to detect onset of delamination in real time", *J. Compos. Mater.* **2014,** *48*, 2175-2189.

23. Karger-Kocsis, J.; Mahmood, H.; Pegoretti, A. "Recent advances in fiber/matrix interphase engineering for polymer composites", *Prog. Mater. Sci.* **2015,** *73*, 1-43.

24. Czigany, T.; Kargerkocsis, J. "Comparison of the failure mode in short and long glass-fiber-reinforced injection-molded polypropylene composites by acoustic-emission", *Polym. Bull.* **1993,** *31*, 495-501.

25. Kargerkocsis, J.; Czigany, T. "Fracture-behavior of glass-fiber mat-reinforced structural nylon RIM composites studied by microscopic and acoustic-emission techniques", *J. Mater. Sci.* **1993,** *28*, 2438-2448.

26. Siegmann, A.; Kander, R.G. "In situ acoustic emission monitoring and mechanical testing in the scanning electron microscope", *J. Mater. Sci. Lett.* **1991,** *10*, 619-621.

27. Chou, H.Y.; Mouritz, A.P.; Bannister, M.K.; Bunsell, A.R. "Acoustic emission analysis of composite pressure vessels under constant and cyclic pressure", *Compos. Part A-Appl. S.* **2015,** *70*, 111-120.

28. Haselbach, W.; Lauke, B. "Acoustic emission of debonding between fibre and matrix to evaluate local adhesion", *Compos. Sci. Technol.* **2003,** *63*, 2155-2162.

29. Al-Jumaili, S.K.; Holford, K.M.; Eaton, M.J.; McCrory, J.P.; Pearson, M.R.; Pullin, R. "Classification of acoustic emission data from buckling test of carbon fibre panel using unsupervised clustering techniques", *Struct. Health Monit.* **2015,** *14*, 241-251.

30. Suresh Kumar, C.; Arumugam, V.; Santulli, C. "Characterization of indentation damage resistance of hybrid composite laminates using acoustic emission monitoring", *Compos. Part B-Eng.*, *in Press*.

31. Karger-Kocsis, J.; Czigany, T.; Mayer, J. "Fracture behaviour and damage growth in knitted carbon fibre fabric reinforced polyethylmethacrylate", *Plast. Rub. Compos. Pro.* **1996,** *25*, 109-114.

32. Czigany, T.; Ostgathe, M.; Karger-Kocsis, J. "Damage development in GF/PET composite sheets with different fabric architecture produced of a commingled yarn", *J. Reinf. Plast. Comp.* **1998,** *17*, 250-267.

33. Benevolenski, O.I.; Karger-Kocsis, J. "Comparative study of the fracture behavior of flow-molded GMT-PP with random and chopped-fiber mats*", Compos. Sci. Technol.* **2001,** *61*, 2413-2423.

34. Benevolenski, O.; Karger-Kocsis, J. "Fracture and failure behavior of partially consolidated discontinuous glass fiber mat-reinforced polypropylene composites (Azdel SuperLite (R))*", Macromol. Symp.* **2001,** *170*, 165-179.

35. Kargerkocsis, J.; Yuan, Q.; Czigany, T. "Assignment of acoustic-emission to the failure sequence and damage zone growth in glass-fiber strand mat-reinforced structural nylon RIM composites*", Polym. Bull.* **1992,** *28*, 717-723.

36. Kargerkocsis, J. "Fracture-mechanical characterization and damage zone development in glass-fiber mat-reinforced thermoplastics*", Polym. Bull.* **1993,** *31*, 235-241.

37. Kargerkocsis, J.; Fejeskozma, Z. "Failure mode and damage zone development in a GMT-PP by acoustic-emission and thermography*", J. Reinf. Plast. Comp.* **1994,** *13*, 768-792.

38. Kargerkocsis, J.; Fejeskozma, Z. "Damage zone development and failure sequence in glass-fiber mat-reinforced polypropylene under static loading conditions*", Mech. Compos. Mater.* **1994,** *30*, 12-18.

39. Karger-Kocsis, J.; Czigany, T. "Effects of interphase on the fracture and failure behavior of knitted fabric reinforced composites produced from commingled GF/PP yarn*", Compos. Part A-Appl. S.* **1998,** *29*, 1319-1330.

40. Romhany, G.; Czigany, T.; Karger-Kocsis, J. "Determination of J-R curves of thermoplastic starch composites containing crossed quasi-unidirectional flax fiber reinforcement*", Compos. Sci. Technol.* **2006,** *66*, 3179-3187.

41. Karger-Kocsis, J. "Swirl mat- and long discontinuous fiber mat-reinforced polypropylene composites - Status and future trends", *Polym. Composite* **2000,** *21*, 514-522.

42. Bailey, P.B.S.; Lafferty, A.D. "Specimen gripping effects in composites fatigue testing - Concerns from initial investigation", *Express Polym. Lett.* **2015,** *9*, 480-488.

43. Ye, X.J.; Zhu, Y.; Yuan, Y.C.; Song, Y.X.; Yang, G.C.; Rong, M.Z.; Zhang, M.Q. "Fatigue life extension of epoxy materials using ultrafast epoxy-SbF5 healing system introduced by manual infiltration", *Express Polym. Lett.* **2015,** *9*, 177-184.

44. Bohse, J. "Acoustic emission examination of polymer-matrix composites", *J. Acoustic Emission* **2004,** *22*, 208-223.

45. Romhany, G.; Szebenyi, G. "Interlaminar crack propagation in MWCNT/fiber reinforced hybrid composites", *Express Polym. Lett.* **2009,** *3*, 145-151.

46. De Rosa, I.M.; Santulli, C.; Sarasini, F. "Acoustic emission for monitoring the mechanical behaviour of natural fibre composites: A literature review", *Compos. Part A-Appl. S.* **2009,** *40*, 1456-1469.

47. Park, J.M.; Kong, J.W.; Kim, J.W.; Yoon, D.J. "Interfacial evaluation of electrodeposited single carbon fiber/epoxy composites by fiber fracture source location using fragmentation test and acoustic emission", *Compos. Sci. Technol.* **2004,** *64*, 983-999.

48. Choi, N.S.; Takahashi, K. "Characterization of the damage process in short-fibre/thermoplastic composites by acoustic emission", *J. Mater. Sci.* **1998,** *33*, 2357-2363.

49. Godin, N.; Huguet, S.; Gaertner, R.; Salmon, L. "Clustering of acoustic emission signals collected during tensile tests on unidirectional glass/polyester composite using supervised and unsupervised classifiers", *Ndt&E Int.* **2004,** *37*, 253-264.

50. Roozen, N.B.; Tazelaar, K.; Koussios, S.; Beukers, A. "A new method to measure critical strain in composite materials - Combining the Euler-Fresnel spiral with acoustic emission to assess crack positions*", Compos. Sci. Technol.* **2014,** *100*, 228-236.

51. Baker, C.; Morscher, G.N.; Pujar, V.V.; Lemanski, J.R. "Transverse cracking in carbon fiber reinforced polymer composites: Modal acoustic emission and peak frequency analysis*", Compos. Sci. Technol.* **2015,** *116*, 26-32.

52. Surgeon, M.; Wevers, M. "Modal analysis of acoustic emission signals from CFRP laminates*", Ndt&E Int.* **1999,** *32*, 311-322.

53. Johnson, M.; Gudmundson, P. "Broad-band transient recording and characterization of acoustic emission events in composite laminates*", Compos. Sci. Technol.* **2000,** *60*, 2803-2818.

54. Lagunegrand, L.; Lorriot, T.; Harry, R.; Wargnier, H.; Quenisset, J.M. "Initiation of free-edge delamination in composite laminates*", Compos. Sci. Technol.* **2006,** *66*, 1315-1327.

55. Oskouei, A.R.; Heidary, H.; Ahmadi, M.; Farajpur, M. "Unsupervised acoustic emission data clustering for the analysis of damage mechanisms in glass/polyester composites*", Mater. Design* **2012,** *37*, 416-422.

56. Liu, P.F.; Chu, J.K.; Liu, Y.L.; Zheng, J.Y. "A study on the failure mechanisms of carbon fiber/epoxy composite laminates using acoustic emission*", Mater. Design* **2012,** *37*, 228-235.

57. Cuadra, J.; Vanniamparambil, P.A.; Hazeli, K.; Bartoli, I.; Kontsos, A. "Damage quantification in polymer composites using a hybrid NDT approach*", Compos. Sci. Technol.* **2013,** *83*, 11-21.

58. Boominathan, R.; Arumugam, V.; Santulli, C.; Sidharth, A.A.P.; Sankar, R.A.; Sridhar, B.T.N. "Acoustic emission characterization of the temperature effect on falling weight impact damage in carbon/epoxy laminates", *Compos. Part B-Eng.* **2014,** *56*, 591-598.

59. Maillet, E.; Baker, C.; Morscher, G.N.; Pujar, V.V.; Lemanski, J.R. "Feasibility and limitations of damage identification in composite materials using acoustic emission", *Compos. Part A-Appl. S.* **2015,** *75*, 77-83.

60. Ferrante, L.; Tirillo, J.; Sarasini, F.; Touchard, F.; Ecault, R.; Urriza, M.A.V.; Chocinski-Arnault, L.; Mellier, D. "Behaviour of woven hybrid basalt-carbon/epoxy composites subjected to laser shock wave testing: Preliminary results", *Compos. Part B-Eng.* **2015,** *78*, 162-173.

61. Petrucci, R.; Santulli, C.; Puglia, D.; Nisini, E.; Sarasini, F.; Tirillo, J.; Torre, L.; Minak, G.; Kenny, J.M. "Impact and post-impact damage characterisation of hybrid composite laminates based on basalt fibres in combination with flax, hemp and glass fibres manufactured by vacuum infusion", *Compos. Part B-Eng.* **2015,** *69*, 507-515.

62. Kakakasery, J.; Arumugam, V.; Rauf, K.A.; Bull, D.; Chambers, A.R.; Scarponi, C.; Santulli, C. "Cure cycle effect on impact resistance under elevated temperatures in carbon prepreg laminates investigated using acoustic emission", *Compos. Part B-Eng.* **2015,** *75*, 298-306.

63. Santulli, C.; Kuan, H.T.; Sarasini, F.; De Rosa, I.M.; Cantwell, W.J. "Damage characterisation on PP-hemp/aluminium fibre-metal laminates using acoustic emission", *J. Compos. Mater.* **2013,** *47*, 2265-2274.

64. Kempf, M.; Skrabala, O.; Altstadt, V. "Acoustic emission analysis for characterisation of damage mechanisms in fibre reinforced thermosetting polyurethane and epoxy", *Compos. Part B-Eng.* **2014,** *56*, 477-483.

65. De Rosa, I.M.; Santulli, C.; Sarasini, F.; Valente, M. "Post-impact damage characterization of hybrid configurations of jute/glass polyester laminates using acoustic emission and IR thermography", *Compos. Sci. Technol.* **2009,** *69*, 1142-1150.

66. De Rosa, I.M.; Santulli, C.; Sarasini, F. "Mechanical and thermal characterization of epoxy composites reinforced with random and quasi-unidirectional untreated Phormium tenax leaf fibers", *Mater. Design* **2010,** *31*, 2397-2405.

67. Hajikhani, M.; Ahmadi, M.; Farjpour, M.; Oskouei, A.R.; Sharifi, A. "Strain energy release rate assessment in mode I delamination of foam core sandwich composites by acoustic emission", *J. Compos. Mater.* **2011,** *45*, 2271-2277.

68. De Rosa, I.M.; Dhakal, H.N.; Santulli, C.; Sarasini, F.; Zhang, Z.Y. "Post-impact static and cyclic flexural characterisation of hemp fibre reinforced laminates", *Compos. Part B-Eng.* **2012,** *43*, 1382-1396.

69. Rios-Soberanis, C.R.; Wakayama, S.; Sakai, T.; Perez-Pacheco, E.; Rodriguez-Laviada, J., Cincinnati, Ohio, USA, 2013.

70. Sarasini, F.; Tirillo, J.; Valente, M.; Ferrante, L.; Cioffi, S.; Iannace, S.; Sorrentino, L. "Hybrid composites based on aramid and basalt woven fabrics: Impact damage modes and residual flexural properties", *Mater. Design* **2013,** *49*, 290-302.

71. Santulli, C.; Sarasini, F.; Tirillo, J.; Valente, T.; Valente, M.; Caruso, A.P.; Infantino, M.; Nisini, E.; Minak, G. "Mechanical behaviour of jute cloth/wool felts hybrid laminates", *Mater. Design* **2013,** *50*, 309-321.

72. Sarasini, F.; Tirillo, J.; Valente, M.; Valente, T.; Cioffi, S.; Iannace, S.; Sorrentino, L. "Effect of basalt fiber hybridization on the impact behavior under low impact velocity of glass/basalt woven fabric/epoxy resin composites", *Compos. Part A-Appl. S.* **2013,** *47*, 109-123.

73. de Vasconcellos, D.S.; Sarasini, F.; Touchard, F.; Chocinski-Arnault, L.; Pucci, M.; Santulli, C.; Tirillo, J.; Iannace, S.; Sorrentino, L. "Influence of low velocity impact on fatigue behaviour of woven hemp fibre reinforced epoxy composites", *Compos. Part B-Eng.* **2014,** *66*, 46-57.

74. Sarasini, F.; Tirillo, J.; Ferrante, L.; Valente, M.; Valente, T.; Lampani, L.; Gaudenzi, P.; Cioffi, S.; Iannace, S.; Sorrentino, L. "Drop-weight impact behaviour of woven hybrid basalt-carbon/epoxy composites", *Compos. Part B-Eng.* **2014,** *59*, 204-220.

75. Mohammadi, R.; Saeedifar, M.; Toudeshky, H.H.; Najafabadi, M.A.; Fotouhi, M. "Prediction of delamination growth in carbon/epoxy composites using a novel acoustic emission-based approach", *J. Reinf. Plast. Comp.* **2015,** *34*, 868-878.

76. Dhakal, H.N.; Sarasini, F.; Santulli, C.; Tirillo, J.; Zhang, Z.Y.; Arumugam, V. "Effect of basalt fibre hybridisation on post-impact mechanical behaviour of hemp fibre reinforced composites", *Compos. Part A-Appl. S.* **2015,** *75*, 54-67.

77. Li, L.; Lomov, S.V.; Yan, X. "Correlation of acoustic emission with optically observed damage in a glass/epoxy woven laminate under tensile loading", *Compos. Struct.* **2015,** *123*, 45-53.

78. Flament, C.; Salvia, M.; Berthel, B.; Crosland, G. "Local strain and damage measurements on a composite with digital image correlation and acoustic emission", *J. Compos. Mater.* **2016,** *50*, 1989-1996.

79. Li, L.; Swolfs, Y.; Straumit, I.; Yan, X.; Lomov, S.V. "Cluster analysis of acoustic emission signals for 2D and 3D woven carbon fiber/epoxy composites", *J. Compos. Mater.* **2016,** *50*, 1921-1935.

80. Kostopoulos, V.; Kotrotsos, A.; Baltopoulos, A.; Tsantzalis, S.; Tsokanas, P.; Loutas, T.; Bosman, A.W. "Mode II fracture toughening and healing of composites using supramolecular polymer interlayers", *Express Polym. Lett.* **2016,** *10*, 914-926.

81. Fotouhi, M.; Najafabadi, M.A. "Acoustic emission-based study to characterize the initiation of delamination in composite materials", *J. Thermoplast. Compos.* **2016,** *29*, 519-537.

82. Shahri, M.N.; Yousefi, J.; Fotouhi, M.; Najfabadi, M.A. "Damage evaluation of composite materials using acoustic emission features and Hilbert transform", *J. Compos. Mater.* **2016,** *50*, 1897-1907.

83. Yousefi, J.; Mohamadi, R.; Saeedifar, M.; Ahmadi, M.; Hosseini-Toudeshky, H. "Delamination characterization in composite laminates using acoustic emission features, micro visualization and finite element modeling", *J. Compos. Mater.* **2016,** *50*, 3133-3145.

84. Monti, A.; El Mahi, A.; Jendli, Z.; Guillaumat, L. "Mechanical behaviour and damage mechanisms analysis of a flax-fibre reinforced composite by acoustic emission", *Compos. Part A-Appl. S.* **2016,** *90*, 100-110.

85. Okafor, A.C.; Otieno, A.W.; Dutta, A.; Rao, V.S. "Detection and characterization of high-velocity impact damage in advanced composite plates using multi-sensing techniques", *Compos. Struct.* **2001,** *54*, 289-297.

86. Ringermacher, H.I.; Knight, B.; Li, J.; Plotnikov, Y.A.; Aksel, G.; Howard, D.R.; Thompson, J.L. "Quantitative evaluation of discrete failure events in composites using infrared imaging and acoustic emission", *Nondestruct. Test. Eva.* **2007,** *22*, 93-99.

87. Scholey, J.J.; Wilcox, P.D.; Wisnom, M.R.; Friswell, M.I. "Quantitative experimental measurements of matrix cracking and delamination using acoustic emission", *Compos. Part A-Appl. S.* **2010,** *41*, 612-623.

88. Ciampa, F.; Meo, M. "A new algorithm for acoustic emission localization and flexural group velocity determination in anisotropic structures", *Compos. Part A-Appl. S.* **2010,** *41*, 1777-1786.

89. Caprino, G.; Lopresto, V.; Leone, C.; Papa, I. "Acoustic Emission Source Location in Unidirectional Carbon-Fiber-Reinforced Plastic Plates with Virtually Trained Artificial Neural Networks*", J. Appl. Polym. Sci.* **2011,** *122*, 3506-3513.

90. Mechraoui, S.E.; Laksimi, A.; Benmedakhene, S. "Reliability of damage mechanism localisation by acoustic emission on glass/epoxy composite material plate*", Compos. Struct.* **2012,** *94*, 1483-1494.

91. Leone, C.; Lopresto, V.; Papa, I.; Caprino, G. "Triangulation method as a valid tool to locate the damage in unidirectional CFRP laminates*", Compos. Struct.* **2012,** *94*, 2418-2423.

92. Crivelli, D.; Guagliano, M.; Eaton, M.; Pearson, M.; Al-Jumaili, S.; Holford, K.; Pullin, R. "Localisation and identification of fatigue matrix cracking and delamination in a carbon fibre panel by acoustic emission*", Compos. Part B-Eng.* **2015,** *74*, 1-12.

93. Al-Jumaili, S.K.; Holford, K.M.; Eaton, M.J.; Pullin, R. "Parameter Correction Technique (PCT): A novel method for acoustic emission characterisation in large-scale composites*", Compos. Part B-Eng.* **2015,** *75*, 336-344.

94. Stepanova, L.N.; Lebedev, E.Y.; Kareev, A.E.; Chaplygin, V.N.; Katarushkin, S.A. "Use of the acoustic emission method in detecting the fracture process in specimens made of composite materials*", Russ. J. Nondestruct+* **2004,** *40*, 455-461.

95. Stepanova, L.N.; Lebedev, E.Y.; Kabanov, S.I.; Chaplygin, V.N.; Katarushkin, S.A.; Ramazanov, I.S.; Kanifadin, K.V. "Study of fracture of specimens made of fiberglass plastic using acoustic-emission and strain measurements*", Russ. J. Nondestruct+* **2009,** *45*, 103-108.

96. Benevolenski, O.I.; Karger-Kocsis, J.; Czigany, T.; Romhany, G. "Mode I fracture resistance of glass fiber mat-reinforced polypropylene composites at various degree of consolidation*", Compos. Part A-Appl. S.* **2003,** *34*, 267-273.

97. Acha, B.A.; Karger-Kocsis, J.; Reboredo, M.M. "Fracture and failure behavior of jute fabric reinforced polypropylene. Effect of the interface modification", *Polym. Polym. Compos.* **2006,** *14*, 483-493.

98. Santulli, C. "Post-impact flexural tests on jute/polyester laminates monitored by acoustic emission", *J. Mater. Sci.* **2006,** *41*, 1255-1259.

99. Santulli, C. "Post-impact damage characterisation on natural fibre reinforced composites using acoustic emission", *Ndt&E Int.* **2001,** *34*, 531-536.

100. Czigany, T. "An acoustic emission study of flax fiber-reinforced polypropylene composites", *J. Compos. Mater.* **2004,** *38*, 769-778.

101. Romhany, G.; Wu, C.M.; Lai, W.Y.; Karger-Kocsis, J. "Fracture behavior and damage development in self-reinforced PET composites assessed by located acoustic emission and thermography: Effects of flame retardant and recycled PET", *Compos. Sci. Technol.* **2016,** *132*, 76-83.

102. Nesvijski, E. "Problems of acoustic sources location in 3D medium", *J. Thermoplast. Compos.* **2005,** *18*, 351-362.

103. Ozevin, D. "Geometry-based spatial acoustic source location for spaced structures", *Struct. Health Monit.* **2011,** *10*, 503-510.

104. Russo, S.; Ghadimi, B.; Lawania, K.; Rosano, M. "Failure analysis using acoustic and energy emission assessment of fibre reinforced polymer material performance under severe conditions", *J. Reinf. Plast. Comp.* **2016,** *35*, 1075-1090.

105. Hill, E.V.K.; Iizuka, J.; Kaba, I.K.; Surber, H.L.; Poon, Y.P. "Neural network burst pressure prediction in composite overwrapped pressure vessels using mathematically modeled acoustic emission failure mechanism data", *Res. Nondestruct. Eval.* **2012,** *23*, 89-103.

106. Dahmene, F.; Yaacoubi, S.; El Mountassir, M.; Bendaoud, N.; Langlois, C.; Bardoux, O. "On the modal acoustic emission testing of composite structure*", Compos. Struct.* **2016,** *140*, 446-452.

107. Han, B.H.; Yoon, D.J.; Huh, Y.H.; Lee, Y.S. "Damage assessment of wind turbine blade under static loading test using acoustic emission*", J. Intel. Mat. Syst. Str.* **2014,** *25*, 621-630.

108. Kirikera, G.R.; Shinde, V.; Schulz, M.J.; Sundaresan, M.J.; Hughes, S.; van Dam, J.; Nkrumah, F.; Grandhi, G.; Ghoshal, A. "Monitoring multi-site damage growth during quasi-static testing of a wind turbine blade using a Structural Neural System*", Struct. Health Monit.* **2008,** *7*, 157-173.

109. Ghoshal, A.; Harrison, J.; Sundaresan, M.J.; Hughes, D.; Schulz, M.J. "Damage detection testing on a helicopter flexbeam*", J. Intel. Mat. Syst. Str.* **2001,** *12*, 315-330.

110. Leone, F.A.; Ozevin, D.; Awerbuch, J.; Tan, T.M. "Detecting and locating damage initiation and progression in full-scale sandwich composite fuselage panels using acoustic emission*", J. Compos. Mater.* **2013,** *47*, 1643-1664.

111. Awerbuch, J.; Leone Jr, F.A.; Ozevin, D.; Tan, T.M. "On the applicability of acoustic emission to identify modes of damage in full-scale composite fuselage structures*", J. Compos. Mater.* **2016,** *50*, 447-469.

112. Assarar, M.; Scida, D.; Zouari, W.; Saidane, E.; Ayad, R. "Acoustic Emission Characterization of Damage in Short Hemp-Fiber-Reinforced Polypropylene Composites*", Polym. Composite* **2016,** *37*, 1101-1112.

113. Assarar, M.; Bentahar, M.; El Mahi, A.; El Guerjouma, R. "Monitoring of damage mechanisms in sandwich composite materials using acoustic emission*", Int. J. Damage Mech.* **2015,** *24*, 787-804.

114. Mohammadi, R.; Najafabadi, M.A.; Saeedifar, M.; Yousefi, J.; Minak, G. "Correlation of acoustic emission with finite element predicted damages in open-hole tensile laminated composites*", Compos. Part B-Eng.* **2017,** *108*, 427-435.